



Characterization of 1La and 1Lb emission from indole-polar solvent complexes by supersonic jet spectroscopy
by Kurt William Short

A thesis submitted in partial fulfillment of the requirements for the degree of Doctor of Philosophy in Chemistry
Montana State University
© Copyright by Kurt William Short (1999)

Abstract:

Two-photon polarized fluorescence • excitation and vibronically resolved one-photon dispersed fluorescence from experiments in the supersonic jet have been used to characterize the lowest excited state of van der Waals complexes of indole and 3-methylindole with various polar solvents. For indole, in complexes with water, methanol, and formamide, the two-photon spectra for all of the complexes have circular/linear polarization ratios of absorptivity (Ω -values) that show the excitation is to the 1Lb state. The Franck-Condon patterns of the dispersed fluorescence for these same indole-polar solvent complexes show that emission is also from the 1Lb state. The complexes of 3-methylindole with water, methanol, ethanol, butanol, diethyl ether, diethylamine, and triethylamine show that the nature of the emitting state is closely related to the proton affinity of the complexing solvent. As the proton affinity increases there appears to be a shift from a 1Lb type excited state to one which has more 1La type characteristics. The point at which the excited state becomes more 1La-like than 1Lb-like appears to be around a proton affinity of 200 kcal/mol. Two-photon Ω -values decrease from 0.99 for water which has a proton affinity of 166.5 kcal/mol to 0.55 for triethylamine which has a proton affinity of 231.2 kcal/mol. The dispersed fluorescence spectra of the 3-methylindole-polar solvent complexes all show characteristics which can be associated with both 1La and 1Lb types of emission. However, for solvents with lower proton affinities the 1Lb type characteristics dominate, while solvents with higher proton affinities have emission more like that expected for the 1La state. Also reported here are results of supersonic jet experiments using 2,3-dimethylindole, 7-azaindole, bare indole, and bare 3-methylindole.

CHARACTERIZATION OF 1L_a AND 1L_b EMISSION FROM INDOLE-POLAR
SOLVENT COMPLEXES BY SUPERSONIC JET SPECTROSCOPY

by

Kurt William Short

A thesis submitted in partial fulfillment
of the requirements for the degree

of

Doctor of Philosophy

in

Chemistry

MONTANA STATE UNIVERSITY-BOZEMAN
Bozeman, Montana

April 1999

D378
Sh811

APPROVAL

of a thesis submitted by

Kurt William Short

This thesis has been read by each member of the thesis committee and has been found to be satisfactory regarding content, English usage, format, citations, bibliographic style, and consistency, and is ready for submission to the College of Graduate Studies.

Patrik R. Callis

Patrik R. Callis 12 Apr 99
Chairperson, Graduate Committee Date

Approved for the Department of Chemistry

David M. Dooley

David M. Dooley 4/12/99
Head, Major Department Date

Approved for the College of Graduate Studies

Bruce McLeod

Bruce L. McLeod 4-16-99
Graduate Dean Date

STATEMENT OF PERMISSION TO USE

In presenting this thesis in partial fulfillment of the requirements for a doctoral degree at Montana State University-Bozeman, I agree that the Library shall make it available to borrowers under rules of the Library. I further agree that copying of this thesis is allowable only for scholarly purposes, consistent with "fair use" as prescribed in the U.S. Copyright Law. Requests for extensive copying or reproduction of this thesis should be referred to University Microfilms International, 300 North Zeeb Road, Ann Arbor Michigan 48106, to whom I have granted "the exclusive right to reproduce and distribute my dissertation in and from microform along with the non-exclusive right to reproduce and distribute my abstract in any format in whole or in part."

Signature

Kurt W. Short

Date

April 12, 1999

The light shines on in darkness,
a darkness that did not overcome it.

John 1:5

To all those who are lights in my life.

ACKNOWLEDGMENTS

As science is ultimately a group endeavor, there are certain individuals I would like to acknowledge and thank, who have helped me over the years in this long process.

I want to thank Dr. Patrik Callis for his patience, encouragement, and concern for my personal well-being in acting as my advisor. Also, I wish to thank Dr. Lee Spangler for his help. He and Pat are most responsible for the chance I was given to come and study in Bozeman.

The other members of my graduate committee, Dr. David Singel, Dr. Jan Sunner, Dr. David Dooley, and Dr. James Dent, are thanked for the gifts of their time and effort in this undertaking.

A large number of other individuals have helped and encouraged me over the years in pursuing my scientific interests, and I wish to acknowledge some of them here. They include Dr. Stephen Thompson, Dr. Robert Woody, Dr. Marshall Fixman, and Coach Jerry Quiller in Fort Collins, the late Dr. Stan Gill in Boulder, Dr. Keith Dunker and Dr. John Bollinger in Pullman, Dr. John Glomset and Dr. Ken Applegate in Seattle, and Dr. Robert Cantor, Dr. Mark Taylor, Dr. Jimmy Tung, Dr. Walter Stockmeyer, and Dr. John Winn in Hanover.

Finally, I want to thank my parents, Don and Marilyn Short, my fellow graduate students, and my friends for their continual support and encouragement, especially Jeff, Brad, John, Mel, Tom and Helen, Kathy and Chuck, Ron, Fr. Bob, Brian, Greg and Pat, and Laura and Jodie.

TABLE OF CONTENTS

	Page
LIST OF TABLES	viii
LIST OF FIGURES	ix
ABSTRACT	xi
INTRODUCTION	1
Motivation for this Research	1
Subject of this Research	9
METHODS	10
Description of Experimental Methods	10
Supersonic Jet	10
Fluorescence Excitation	12
Dispersed Fluorescence	13
Polarized Two-Photon Excitation	13
Materials and Experimental Procedures	18
Chemicals and Materials Used	18
Instrumentation	19
Calculations	22
Computer Hardware	22
Computer Software	22
Spectral Simulations	23
RESULTS AND DISCUSSION	25
Indole-Polar Solvent Complexes	25
Indole-Water	25
Indole-Methanol	32
Indole-Formamide	37
Simulation of Spectra	37
Origin of Broad Redshifted Emission	39
Consideration of Exciplexes	40
Summary of the Evidence of ¹ L _b Emission	41
3-Methylindole-Polar Solvent Complexes	42
Fluorescence Excitation	42
Two-Photon Excitation	45
Dispersed Fluorescence	45
Further Characterization of the Higher Vibronic Levels of the Water, Methanol, Ethanol, and Triethylamine Complexes	47
Simulated versus Experimental Dispersed Fluorescence	55
Ab Initio versus Experimental Spectra	57
The Effects of Solvent Proton Affinity	59

A Model for Solvent Changes in Emission	61
2,3-Dimethylindole	63
Fluorescence Excitation	64
Two-Photon Results	65
Dispersed Fluorescence	69
Water Complexes	69
7-Azaindole	72
Other Dispersed Fluorescence Results	75
Bare Indole	76
Bare 3-Methylindole	78
SUMMARY AND CONCLUSIONS	84
REFERENCES CITED	86
APPENDICES	90
A. Dispersed Fluorescence of Indole	91
B. Dispersed Fluorescence of 3-Methylindole	121
C. Dispersed Fluorescence of 2,3-Dimethylindole	125
D. Computer Programs	128

LIST OF TABLES

Tables	Page
1. Temperatures used in the Jet Experiments	21
2. Tentative Assignment of Intramolecular Indole-Water Vibrations	31
3. Assignment of Progressions for the 3-Methylindole Complexes	43
4. 3-Methylindole Complexes, Proton Affinities, and Ω -Values	47
5. 2,3-Dimethylindole, Fluorescence Excitation	66
6. Corresponding Ground and Excited State Frequencies, 3-Methylindole	83

LIST OF FIGURES

Figures	Page
1. Structure of Indole Derivatives	2
2. Resolution of 1L_a and 1L_b Bands	3
3. Permanent Dipoles of Indole	4
4. Diagram of the Supersonic Jet	10
5. Energy Representation of Fluorescence Methods	12
6. Experimental Setup	19
7. Method of Spectral Simulation	23
8. Fluorescence Excitation, Indole H ₂ O Complex	25
9. Indole-Water, Two-Photon Excitation	26
10. Dispersed Fluorescence, Indole-Water	28
11. Intramolecular Vibrations, Indole-Water	30
12. Fluorescence Excitation, Indole, Specific Detection	32
13. Fluorescence Excitation, Indole:MeOH Complex	33
14. Indole-Methanol, Two-Photon Excitation	34
15. Indole-Methanol, Dispersed Fluorescence	35
16. Indole-Methanol, Dispersed Fluorescence, Difference Spectrum	36
17. Indole-Formamide	38
18. Indole-Water, Simulated Spectra	40
19. Fluorescence Excitation, 3-Methylindole Complexes	44
20. Polarized Two-Photon Excitation, 3-Methylindole Complexes	46
21. Dispersed Fluorescence, 3-Methylindole Complexes	48
22. Dispersed Fluorescence, 3-Methylindole, 3-Methylindole-Water	49
23. Two-Photon Excitation, 3-Methylindole-Water	51
24. Two-Photon Excitation, 3-Methylindole-Methanol	52

LIST OF FIGURES-Continued

Figures	Page
25. Two-Photon Excitation, 3-Methylindole-Ethanol	53
26. Two-Photon Excitation, 3-Methylindole-Triethylamine	54
27. Dispersed Fluorescence, Simulated 3-Methylindole-Water, Experimental 3-Methylindole-Water	56
28. Dispersed Fluorescence, 3-Methylindole-Diethylamine, 3-Methylindole ¹ L _a Ab Initio Results	58
29. Ω-Value vs. Proton Affinity	60
30. Fluorescence Excitation, 2,3-Dimethylindole	67
31. Two-Photon Excitation, 2,3-Dimethylindole	68
32. Dispersed Fluorescence, 2,3-Dimethylindole	70
33. Fluorescence Excitation, 2,3-Dimethylindole-Water	71
34. Dispersed Fluorescence, 2,3-Dimethylindole-Water	73
35. 7-Azaindole, Fluorescence Excitation, Dispersed Fluorescence	74
36. 7-Azaindole-Water, Fluorescence Excitation, Dispersed Fluorescence	75
37. Dispersed Fluorescence, Indole, 1095, 1120, 1284, 1329, and 1357 cm ⁻¹	77
38. Dispersed Fluorescence, 3-Methylindole, 408, 419, 427, and 467 cm ⁻¹	81
39. Dispersed Fluorescence, 3-Methylindole, 608, 617, 713, and 738 cm ⁻¹	82
40. Dispersed Fluorescence, 3-Methylindole, Expanded View	83

ABSTRACT

Two-photon polarized fluorescence excitation and vibronically resolved one-photon dispersed fluorescence from experiments in the supersonic jet have been used to characterize the lowest excited state of van der Waals complexes of indole and 3-methylindole with various polar solvents. For indole, in complexes with water, methanol, and formamide, the two-photon spectra for all of the complexes have circular/linear polarization ratios of absorptivity (Ω -values) that show the excitation is to the 1L_b state. The Franck-Condon patterns of the dispersed fluorescence for these same indole-polar solvent complexes show that emission is also from the 1L_b state. The complexes of 3-methylindole with water, methanol, ethanol, butanol, diethyl ether, diethylamine, and triethylamine show that the nature of the emitting state is closely related to the proton affinity of the complexing solvent. As the proton affinity increases there appears to be a shift from a 1L_b type excited state to one which has more 1L_a type characteristics. The point at which the excited state becomes more 1L_a -like than 1L_b -like appears to be around a proton affinity of 200 kcal/mol. Two-photon Ω -values decrease from 0.99 for water which has a proton affinity of 166.5 kcal/mol to 0.55 for triethylamine which has a proton affinity of 231.2 kcal/mol. The dispersed fluorescence spectra of the 3-methylindole-polar solvent complexes all show characteristics which can be associated with both 1L_a and 1L_b types of emission. However, for solvents with lower proton affinities the 1L_b type characteristics dominate, while solvents with higher proton affinities have emission more like that expected for the 1L_a state. Also reported here are results of supersonic jet experiments using 2,3-dimethylindole, 7-azaindole, bare indole, and bare 3-methylindole.

INTRODUCTION

Motivation for this Research

The spectroscopic characterization of proteins and their components has long been a subject of great interest to physical and biological scientists. This interest is the result of the belief that it should be possible to determine much about the structure and local environment in a protein simply from the intensity, shape, and wavelength of the spectral signal. All of the amino acids in proteins show spectroscopic activity. However, of the twenty amino acids that commonly make up proteins, tryptophan has been of greatest importance in probing local protein structure and environment. This is because tryptophan has by far the largest spectroscopic activity (absorption) in the near UV (250-300nm) (1), and because it has the most sensitivity to changes in the local environment. So, even if a large protein contains only one tryptophan residue, it will dominate the protein spectrum in this wavelength range. The intensity and wavelength position of the maximum fluorescence signal will depend strongly on the local environment and conformation of the tryptophan residue. Thus, tryptophan (or one of its analogues) can be used as a sensitive local probe in proteins. In many instances, this is accomplished by using site specific mutagenesis in which specific insertions or deletions of tryptophan are made. For this reason, it is important to determine what changes in tryptophan fluorescence mean in terms of specific changes in its local environment and conformation.

In the absorption spectrum of aqueous tryptophan three of the important (π, π^*) transitions occur at about 220nm (45455cm^{-1}), 280nm (35714cm^{-1}), and 288nm (34722cm^{-1}) {439}. These correspond

respectively to the electronic transitions ${}^1B_a \leftarrow {}^1A$, ${}^1L_a \leftarrow {}^1A$, and ${}^1L_b \leftarrow {}^1A(2,3)$. The same three bands are also present in solution spectra of indole, which is the chromophore of tryptophan (see Figure 1).

Structures of Indole Derivatives

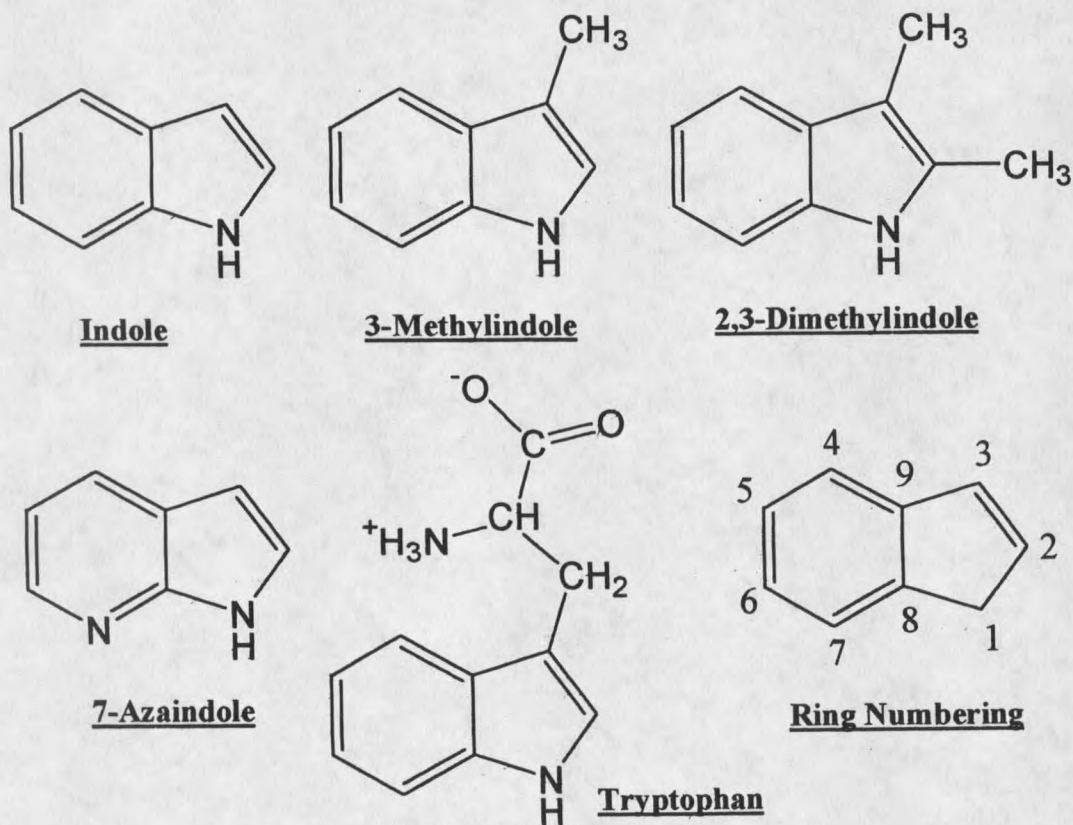


Figure 1. The structures of various indole derivatives and the numbering of the indole ring are shown.

Their exact positions depend on the particular indole derivative and the polarity of the solvent environment. We are interested here in the nearly degenerate 1L_a and 1L_b transitions. For many indole derivatives in polar solutions(4) or low temperature solvent glasses(5-7), absorption spectra show that the 1L_a maximum occurs at higher energy than the 1L_b maximum. However, the 1L_a band often has a low energy tail

that extends beyond the red edge of the 1L_b transition (Figure 2). The work described in this thesis has helped to firmly establish the view that, for most proteins, the 1L_a 0-0 transition occurs at a lower energy than the 1L_b 0-0 transition(8).

Resolution of 1L_a and 1L_b Bands

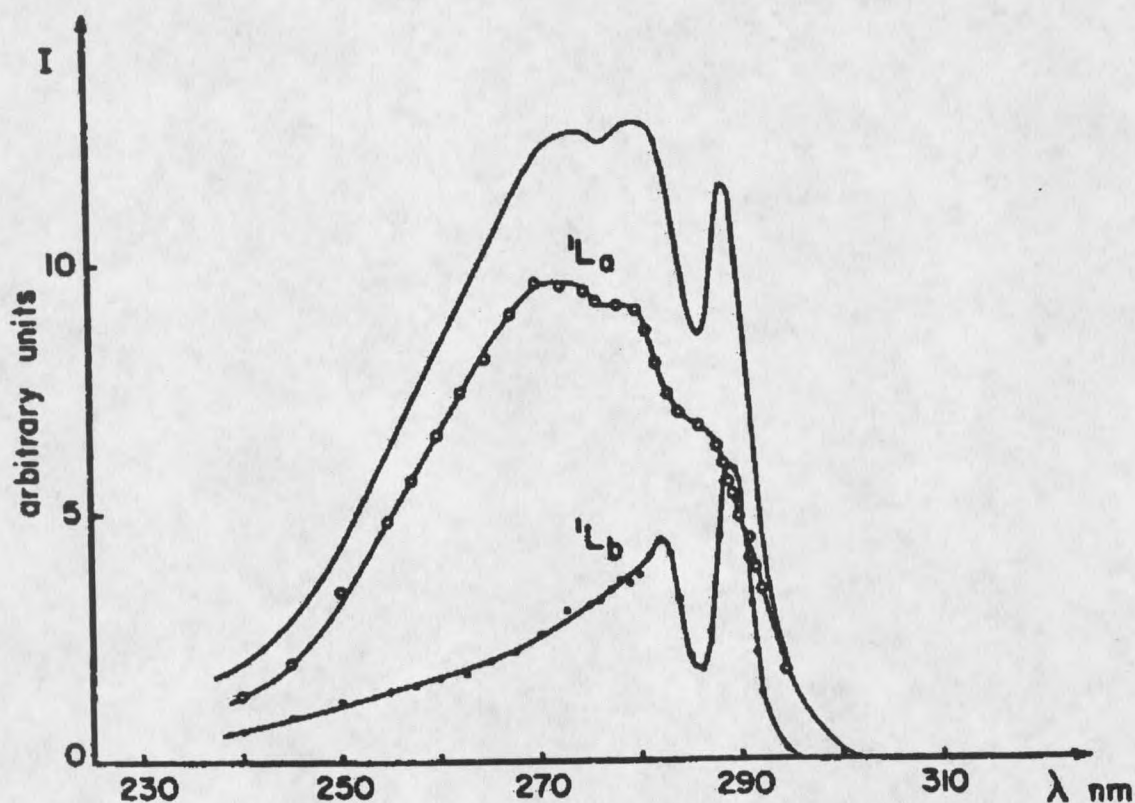


Figure 2. The absorption spectrum of indole is shown resolved into its 1L_a and 1L_b components. This figure is taken from reference(6).

The fluorescence spectrum of indole is extremely sensitive to the polarity of its environment. The spectral position of 1L_a emission is particularly sensitive to local environment. This is due to the large permanent dipole moment of this state. The larger dipole will have more interaction with the local electric field caused by the neighboring atoms, stabilizing or destabilizing the excited state that affects the properties of the fluorescence(9). The magnitude and directions of the

ground, 1L_a , 1L_b , and 3L_a permanent dipoles are shown in figure 3. The ground state dipole has a value of 2.1D, the 1L_a 5.1D, and the 1L_b 2.2D(2). More recent measurements have put the ground state to excited state permanent dipole changes at $^1L_a|\Delta\mu|=5.9\pm 0.3D$ and $^1L_b|\Delta\mu|=1.3\pm 0.3D(10)$. So, it is not surprising that the spectral position of 1L_a emission is very sensitive to its environment.

Permanent Dipoles of Indole

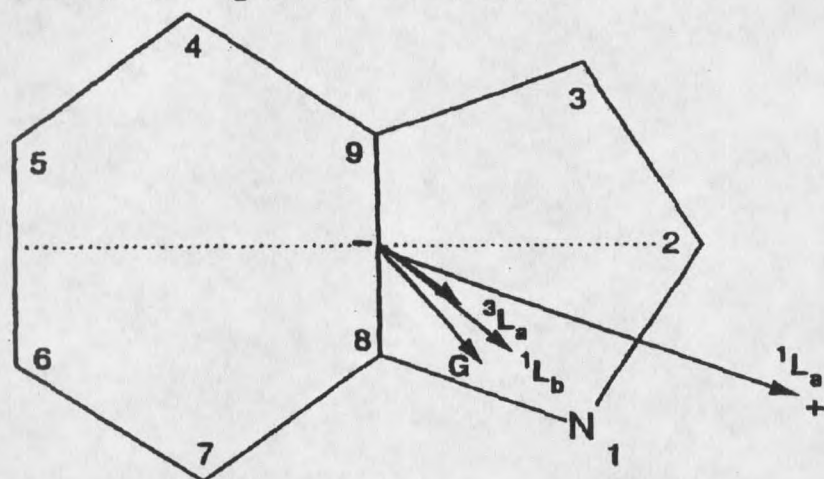


Figure 3. The 1L_a , 1L_b , 3L_a , and ground state(G) permanent dipoles of indole are shown. This figure is taken from reference(9).

This sensitivity to environment makes indole amenable to studies in which it is formed into van der Waals complexes with various solvents in the environment of a supersonic jet. Jet spectroscopy allows high resolution vibronically (and rotationally) resolved spectra to be collected in the gas phase. Its characteristics will be reviewed in the Experimental section. Since complexes can be formed that contain only one or two solvent molecules, it is possible to determine how specific solvent interactions affect 1L_a and 1L_b emission. Information of this type will be very important in establishing how specific interactions in proteins affect tryptophan fluorescence.

Various derivatives of indole can be formed by attaching substituents at different positions around the five- or six-membered rings. Addition at each position affects the fluorescence emission in different ways(5). It is important to understand these changes in fluorescence for the following reasons. First, for tryptophan in proteins the connection of the indole group to the peptide backbone is via the 3-position, thus 3-methylindole is the indole analogue most like tryptophan. Second, it has recently become possible to incorporate tryptophan analogues into proteins in place of unmodified tryptophan. These analogues include 7-azaindole(11) and 4-fluoroindole(12). Since these modified tryptophans can be used as reporter groups in proteins it is important to understand their spectroscopic properties. Finally, it is interesting from a fundamental point to understand how an identical perturbation at different ring positions affects indole fluorescence. The mono-methylated indoles have been useful in this regard(5).

Jet spectroscopy measurements of indole have characterized the vibronic structure of both the ground(13) and excited states(14). Using only jet data, it initially proved impossible to determine the location of the 1L_a origin(15-18). However, the combination of polarized two-photon jet spectra with matrix isolation studies of indole in an argon matrix(19), has found the location of the 1L_a origin of indole to be displaced about 1400 cm^{-1} above that of the 1L_b origin. This is in agreement with the seminal work done by Strickland et.al.(20) more than twenty-five years ago on indole dissolved in polar and non-polar solvents.

The maximum wavelength of tryptophan fluorescence in proteins, in solution, varies from 308-355nm, depending primarily on the exposure of the indole chromophore to water(8,21-25). Therefore, of the jet studies that have been done on indole and its various derivatives in van der

Waals complexes with one or more polar or non-polar solvent molecules(16,17,26-36), the ones involving water complexes(16,26,28-34,36) have been of most interest. Hager et al. first reported that indole formed two van der Waals complexes with water(30) and alcohols(31): one whose origin was shifted 132-214 cm^{-1} below the bare molecule origin(the σ -complex), and another whose origin was shifted 450-518 cm^{-1} below the bare origin and showed greater Franck-Condon(FC) activity. The σ -complex was assigned to a complex in which the solvent acted as a proton acceptor from the indole NH group. The second complex was at first attributed to an indole associated with two solvent molecules because of its concentration dependence(31), but the subsequent observation that this signal was confined to the indole + H_2O mass channel during mass selected experiments(30) led to its assignment as a second 1:1 complex. Because no redshifted complexes were found for N-methylindole, Hager et al. suggested that the second 1:1 complex also involved a hydrogen bond with the water or methanol acting as a proton acceptor(30). Levy and co-workers(35,37) then discovered that a special conformer of tryptophan and related molecules exhibited a long FC progression in a 20-30 cm^{-1} vibration in the excitation spectrum, and that excitation of the special conformer resulted in a unique redshifted and diffuse dispersed fluorescence in comparison to that from other conformers. In the course of their extensive investigation, the Levy group came to the interpretation that this behavior was associated with an intramolecular π -complex between a polar side chain and the indole π system. They also concluded (despite no real proof) that the interaction was sufficient to invert the order of the nearly degenerate 1L_a and 1L_b $\pi\pi^*$ excited states whose mixing was responsible for the large FC activity and the diffuse redshifted fluorescence. This interpretation was then extended to those complexes of indole with water, methanol,

formamide, and acetamide that exhibited long, low-frequency progressions and broad, redshifted fluorescence(29). Independently, Arnold and Sulkes(28,36) applied the same interpretation to a larger set of methylated indoles complexed with various polar molecules, concluding that solvent-induced 1L_a emission in jet-cooled indole complexes is more the rule than the exception. Finally, the Levy group(29) tried to correlate the two types of complexes observed in cold jets with the two exciplexes postulated by Lumry and co-workers(38,39) to explain the pronounced redshifts of fluorescence for solutions of indole in hydrocarbons at room temperature when mM quantities of alcohols were added.

An achievement of this thesis has been to show unequivocally that the above picture is incorrect. We have used polarized two-photon excitation and dispersed fluorescence, to show that jet-cooled complexes of indole with the polar solvents water, methanol, and formamide are both excited to and emit from the 1L_b state. We have also shown that exciplexes are not involved in the redshifted indole polar-solvent complexes.

Despite no real proof of its structure, it has become well accepted to refer to the indole-water complex with the redshifted spectrum as the π -complex(28,29,36). Recently, however Carney, Hagemeister, and Zwier, have found from resonant ion-dip infrared spectra, infrared-ultraviolet holeburning, and supporting *ab initio* calculations(40) that this complex has the formula indole-(H₂O)₂, with one water accepting a hydrogen bond from the indole N-H and the other accepting a hydrogen bond from the first water and bridging to the π -system. Because of this, the complexes showing redshifted spectra will be referred to as " ρ -complexes," with the " ρ " standing for redshifted. This red shift is what the indole-polar

solvent complexes have in common with the intramolecular complexes reported by the Levy group.

Although fluorescence from some complexes of different indole derivatives with polar solvents is believed to originate in the 1L_a state, one question has remained. What is the vibronic structure of 1L_a fluorescence in a jet environment? It was originally suggested, based on the unexpectedly short fluorescence lifetimes for the higher vibronic modes of 2,3-dimethylindole(13,28,33), that the 1L_a transitions could not be observed in the jet because this state is dissociative through breaking of the N-H bond. Further studies with 3-methylindole(34) and negative results in a mass-resolved search for the possible fragment of N-H bond dissociation in 2,3-dimethylindole(36), led to the suggestion that the 1L_a state is not dissociative, but is coupled to a third state that is probably a highly excited ground state vibronic level. So the short lifetimes in 2,3-dimethylindole were explained by non-radiative decay to this state. Independent of this idea, as mentioned above, the idea that emission from the 1L_a state is broad and redshifted was being proposed(28,29,36). During this same time, experimental and theoretical results from the Callis group had started to suggest a slightly different picture of 1L_a emission. Muñio and Callis(32) showed that dispersed fluorescence from an indole-H₂O complex, that was believed to originate from the 1L_a state, could be well represented simply by adding the appropriate progression onto each line of the emission spectrum from bare indole(which has 1L_b emission) and broadening each line by 50 cm⁻¹ to simulate typical monochromator resolution. This suggested that the emission could not be 1L_a because it was constructed from 1L_b emission. Also, *ab initio* calculations of the vibronic spectra for indole(41) had suggested that 1L_a emission while different from 1L_b emission should have a well defined vibronic structure in which the 0-0 transition and should

have the largest FC activity. Initial experimental evidence for these ideas has come from well resolved phosphorescence spectra of indole in an argon matrix(42). Indole phosphorescence is known to originate from the 3L_a state and so should have a FC pattern very similar to that expected for 1L_a fluorescence. This is exactly what was found for the 3L_a phosphorescence spectrum of indole. It is against this background that the research to be presented here was started.

Subject of this Research

The research described here was started at a time when the nature of the emission from the ρ -complex was undefined. A major goal was to clearly define the state to which this complex was excited and from which it emitted, using polarized two-photon excitation and high resolution dispersed fluorescence. It should be noted that the sensitivity of the measurements had to be extended well beyond what had been previously obtained in our lab(two-photon measurements) or in other labs(dispersed fluorescence).

Another goal in this research was to more clearly define the vibronic structure of the $^1L_a \leftarrow$ ground transition and to prove that it can be observed in the supersonic jet. Also we wanted to form a better picture of the way in which polar solvents influence the energies of the 1L_a and 1L_b states relative to one another. This has been done by studying 3-methylindole in the supersonic jet, either as a bare molecule or as a van der Waals complex with polar solvent molecules.

METHODS

Description of Experimental Methods

There were three different spectroscopic methods used in these studies. They are fluorescence excitation, dispersed fluorescence, and polarized two-photon excitation. All measurements were made after laser excitation of the sample in a supersonic jet apparatus. The jet setup will be described first, then the three different experimental methods will be reviewed.

Supersonic Jet

Jet spectroscopy and the advantages derived using this method are based on some very simple ideas. A diagram of the jet apparatus is shown in Figure 4.

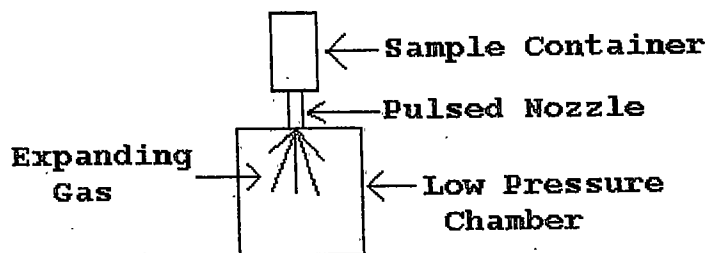
Diagram of the Supersonic Jet

Figure 4. A diagram of the supersonic jet setup is shown.

The sample container is pressurized with the sample and a carrier gas (normally helium, although other noble and non-noble gases can be used) at a pressure of 0.5atm (about 380 torr) or greater. This chamber is connected to a second chamber maintained at low pressure (10^{-5} torr or

less) by a small diameter (0.05 to 1mm) opening or nozzle that may or may not be pulsed, to allow gas passage from the higher pressure to lower pressure chamber. As the sample and carrier gas expand into the low pressure chamber there are a large number of collisions while exiting the nozzle, in the early stages of the expansion. It is this process that causes the "cooling" characteristic of jet spectra. The mechanism involves collisional energy exchange that converts the random thermal energy of the gas in the high pressure chamber into directed energy of flow in the expansion. This will continue as long as the gas density in the expansion is high enough to support collisions, and the temperature will continue to drop. If a polyatomic molecule, such as indole, is included in the expansion there will be a collisional exchange of energy between the translationally cold carrier gas and the vibrational and rotational modes of the polyatomic molecule. When gas density falls below the level necessary to support collisions, the vibrational and rotational temperatures become frozen at specific values. It is common to obtain rotational temperatures of 5K and vibrational temperatures below 50K(43). This restricts populations of rotational levels to within 3 to 4 cm^{-1} of the ground rotational level, and of vibrational states to levels with less than 30 to 40 cm^{-1} of vibrational energy. The low rotational temperature causes vibrational lines in the spectra to be very narrow and the low vibrational temperature causes most transitions to originate from the $v=0$ level of the ground electronic state. This allows jet spectra to have well resolved vibrational lines and allows these transitions to be more easily assigned to specific normal modes in the excited state.

Fluorescence Excitation

One simple experiment that gives information about the structure of the excited state is fluorescence excitation. In the jet this experiment involves excitation, with a single photon of light, from the lowest vibrational level of the ground state to the vibrational levels of an upper state. The total fluorescence from each of these levels is monitored (see Figure 5). Because of the cooling that takes place in the jet, the lines are usually narrow and well resolved. The information obtained from fluorescence excitation is the same as that from absorption spectroscopy except that the sensitivity is much greater than with absorption measurements.

Energy Representation of Fluorescence Methods

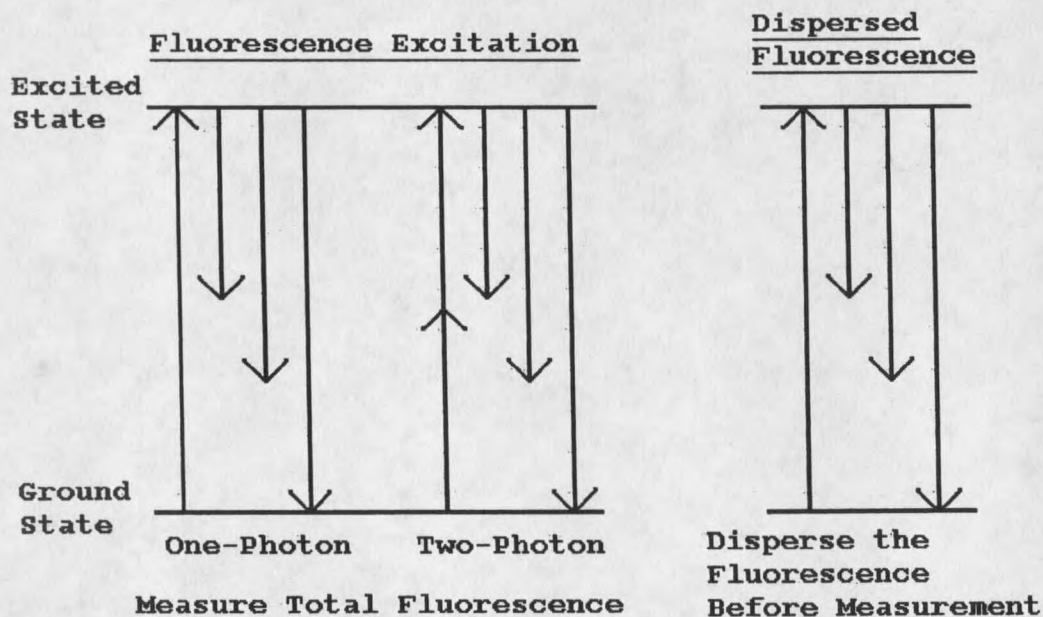


Figure 5. A schematic representation of one- and two-photon fluorescence excitation, and of dispersed fluorescence is shown.

Dispersed Fluorescence

Another one photon experiment, gives information about the energy distribution of the ground state vibrational levels, is dispersed fluorescence. In this experiment, a specific vibrational level of an upper electronic state is excited and the vibrationally resolved emission spectrum of the ground state is collected (see Figure 5). The information gained from the spectra can in many cases be used to correlate one or more specific vibrational levels in the ground state with a specific excited state level. As will be shown below, dispersed fluorescence is also somewhat useful in helping to decide whether emission is from the 1L_a or 1L_b states.

Polarized Two-Photon Excitation

A different way to excite a molecule from the ground state to a higher electronic level is through multiphoton excitation. We are interested here in polarized two-photon excitation. This type of spectroscopy is actually a three-photon process because, not only are two photons needed to reach a higher state, but a third photon is emitted as the molecule relaxes back to the ground state (see Figure 5). The first two photons can be either of the same or different energies. Their absorption occurs in about 10^{-16} seconds (44), and so the molecule is essentially motionless during the process. In the studies here, we also assume that there is complete randomization of the gas phase molecules before emission of the fluorescence photon. Thus, there is no polarization information to be gained. There is however a conservation of information about the original excited state, even if the molecule undergoes internal conversion to another excited state before emitting (45).

The two-photon effect was first proposed by Göppert-Mayer in 1931(46). At that time however, there were no high-intensity light sources with which to test it. With the advent of lasers, experimental applications have increased. In tandem the theoretical treatment has also improved. The series of articles by McClain and coworkers(45,47-49) as well as recent treatments by Callis(44,50), are useful in understanding two-photon spectroscopy. Since these published descriptions of two-photon absorption are quite well written and informative, a detailed treatment will not be given here. However, it is useful to review some of the more important points.

The rate at which two photons can be absorbed by a molecule is represented by the following equation(49).

$$\text{Rate} = 128\pi^3\alpha^2\omega^2g_m(2\omega)|\boldsymbol{\mu} \cdot \mathbf{S} \cdot \boldsymbol{\mu}|^2\phi^2$$

Where $\boldsymbol{\mu}$ is the unit polarization vector of the exciting light, \mathbf{S} is the two-photon tensor, ϕ is the flux of the excitation light, α is the fine-structure constant, and $g_m(2\omega)$ is the line-shape function. One thing to note is that the rate is proportional to the light intensity squared. This explains why light sources with high photon fluxes are so useful in two-photon spectroscopy.

The two-photon tensor, \mathbf{S} , is given by(49)

$$\mathbf{S} = \sum_i \frac{r_{fi}r_{ig}}{\nu_{ig} - \nu_{\text{laser}}}$$

Or in terms of Cartesian components of the 3 x 3 matrix, one component S_{ab} is

$$S_{ab} = \sum_i \frac{a_{fi} b_{ig}}{\nu_{ig} - \nu_{laser}}$$

Where $a, b = x, y, z$. $r_{fi} r_{ig}$ and $a_{fi} b_{ig}$ are the product of the transition dipole between the initial state, g , and any of the states of the molecule, i , times the transition dipole from state i to the final state, f . ν_{ig} is the frequency difference between the ground state and any of the states of the molecule, and ν_{laser} is the frequency of the exciting light. A two-photon absorption event will then usually have no direct relationship to the transition dipole for one-photon absorption directly to the same final state.

The fluorescence intensity for emission of a single photon after absorption of two photons is given by

$$I = \sum_{i,j=1}^4 P_i M_{ij} Q_j$$

where P_i are geometric factors depending on the polarization of the absorbed and emitted photons, Q_j are molecular factors that depend on the two-photon absorption tensor and the fluorescence transition dipole, and M_{ij} are the components of the averaging matrix that connect the geometric and molecular factors. One of the Q_j factors, Q_3 or Q_Y , is directly connected to an easy to measure experimental parameter known as the two-photon polarization, Ω . Q_Y is the square of the normalized two-photon tensor. The relationship is summarized in the following equations (44). First,

$$Q_3 \equiv Q_Y = \frac{\delta_F}{\delta_G}$$

where

$$\delta_G = \sum_{a,b} S_{ab} S_{ab}^* = |\mathbf{S}|^2 \quad \text{and} \quad \delta_F = \sum_{a,b} S_{aa} S_{bb} = |\text{Tr} \mathbf{S}|^2$$

The ratio δ_F/δ_G is measured experimentally when the emission is isotropic by the two-photon polarization, Ω , where

$$\Omega = \left(\frac{\delta_{\text{circular}}}{\delta_{\text{linear}}} \right)_{\text{isotropic}} = \frac{3 - \delta_F/\delta_G}{2 + \delta_F/\delta_G}$$

or

$$Q_Y = \frac{\delta_F}{\delta_G} = \frac{3 - 2\Omega}{1 + \Omega}$$

Here, δ_{circular} and δ_{linear} are the absorptivities from excitation with circular and linearly polarized light, respectively. Experimentally, Ω is found by determining ratio of the areas under the peaks from the total fluorescence by two-photon excitation with circularly and linearly polarized light. Knowledge of Q_Y is important in the two-dimensional limit. The indole chromophore falls under this limit since the electronic transitions are within the plane of the molecule. Given Q_Y it is possible to determine the maximum and minimum values of the anisotropy, r_{\pm} , by

$$r_{\pm} = \frac{2 \pm 9 \left[Q_Y (2 - Q_Y) \right]^{1/2} + Q_Y}{14 + 7Q_Y}$$

This provides a direct connection between gas-phase experiments and experiments in which the anisotropy can be measured directly.

For isotropic emission, Ω can vary only from 0 to 3/2. For pure 1L_a emission from indole, Ω has a value of about 0.5 and for pure 1L_b emission from indole Ω has a value of 1.4(44). Since the angle between the 1L_a and 1L_b transition dipoles of 3-methylindole is similar to that

of indole(5), it is assumed that the electronic properties of 3-methylindole are similar to those of indole. Also, the calculated two-photon tensor shapes for the 1L_a and 1L_b transitions of 3-methylindole are similar to those of indole(50), so the Ω -values for 1L_a and 1L_b emission are expected to be similar for the two molecules. This is not quite what is found experimentally. For excitation to the 1L_b state, $\Omega \approx 1.4$ for indole(4) and $\Omega \approx 1.13$ for 3-methylindole(51). For emission when excitation is to the 1L_a state, $\Omega \approx 0.5$ for both indole and 3-methylindole(4).

Finally, as stated above, information about the two photon polarization in absorption is preserved regardless of the mode of excited state decay. In two-photon experiments there is preferential excitation of the 1L_a state by linearly polarized light and of the 1L_b state by circularly polarized light. One way to understand this is to consider the value of Q_Y , the normalized trace squared of an \mathbf{S} tensor with no off-diagonal elements. The shape of the tensor changes as Q_Y changes, thus changing the polarization of light favored for excitation. For the 1L_b state ($\Omega=1.4$) the tensor has a near zero Q_Y value, which favors excitation by light that is circularly polarized (or two linear photons with perpendicular polarizations). For the 1L_a state ($\Omega=0.5$) the tensor has relative principal values of 1.0, 0.17, and 0.0, that favor excitation by light that is linearly polarized. It is shown that these are the correct values by substituting $\Omega=0.5$ into the equation for Q_Y to obtain $Q_Y = \delta_F / \delta_G = 1.33$. It can then be shown that if the xx , yy , and zz elements of the tensor (with no off-diagonal elements) are 1.0, 0.17 and 0.0 respectively, then δ_F will equal 1.3689 and δ_G will equal 1.0289. These are the values which give $Q_Y=1.33$.

The preferential excitation, based on the polarization of the light used, is an advantage that two-photon polarization measurements have over one-photon polarization measurements. In one-photon gas phase experiments it is not possible to gain information about which state the excitation is to, because it is not possible to directly measure the anisotropy.

Materials and Experimental Procedures

Chemicals and Materials Used

Indole (99+%, lot numbers 03231AZ and 14818CG), 3-methylindole (98%, lot number 08810LQ), 2,3-dimethylindole (97+%, lot number 092767), and 7-azaindole (98%, lot number 05026LG) from Aldrich were used without further purification. For indole, bulk deionized water, methanol (HPLC grade) from Fisher, and formamide (Practical grade) from E. M. Science were used in forming the complexes. For 3-methylindole, bulk deionized water, spectroscopic grade methanol from J. T. Baker Chemical Company, ethanol from U.S. Industrial Chemicals Co. (dehydrated), freshly redistilled diethylether, diethylamine (99%+) from Acros, and triethylamine (99%) from Acros were used in forming the complexes. For 2,3-dimethylindole and 7-azaindole, bulk deionized water was used in forming the complexes. Ultra-pure helium (99.999%), from General Distributing Co. (in Bozeman, MT) was used as a carrier gas in the jet. The laser dyes rhodamine choride 560, rhodamine tetrafluoroborate 590, rhodamine perchlorate 610, rhodamine perchlorate 640, and coumarin 540A were from Exciton. Bulk grade methanol from Dyce Chemical Company (Billings, MT) was used as a solvent for the dyes. Often, a mixture of more than one dye was used in order to get maximum laser intensity in a desired frequency range. Glass filters were from Schott Glass Technologies.

Instrumentation

The experimental setup is shown in Figure 6.

Experimental Setup

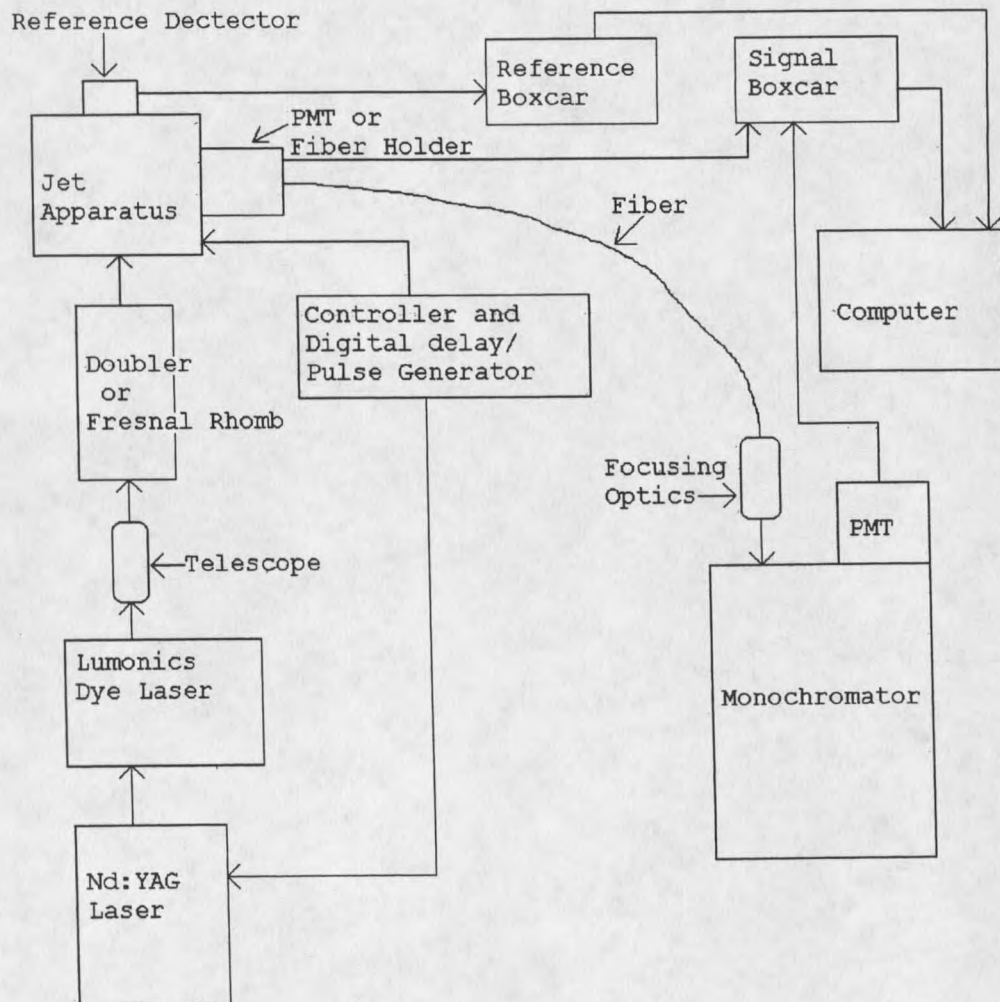


Figure 6. The experimental setup is shown.

A Lumonics HD300 dye laser was pumped with either a Lumonics Nd:YAG (HY-200) at 20 Hz or a Continuum Surelite III Nd:YAG at 10 Hz. Pulse lengths are about 8ns for the Lumonics Nd:YAG laser and 3-5ns for the

Continuum laser. The energy of a pulse from the dye laser was dependent on the dye(s) used, its age, and how hard it was pumped. With the Continuum laser, running at 532nm, the flashlamp voltage was normally 1.28-1.38kV for one-photon experiments and 1.48-1.55kV for two-photon experiments. Depending on the experiment, either the third harmonic (355 nm) or the second harmonic (532 nm) were used to pump the dye laser. The supersonic jet is the same setup that has been described before(52). For one-photon fluorescence excitation experiments and dispersed fluorescence experiments an INRAD Autotracker II frequency doubler was used to generate ultraviolet light. The doubled light was passed through UG-11 filter (1 mm thick) to prevent transmission of the fundamental. During two-photon experiments the light was not doubled, but a double Fresnel rhomb half-wave plate followed by a Fresnel rhomb were used to generate circular and linear polarizations for the spectra.

The indoles were placed in a heated sample chamber. The jet nozzle was kept at 5-20 °C above the sample chamber in order to inhibit clogging of the nozzle tip. Temperatures used in the experiments are shown in Table 1.

Backing pressures between 0.0 and 2.7 atm were used in all experiments. The pressure of 0.0 atm was used when the nozzle was shut off in order to collect background fluorescence. The nozzle was driven and the laser triggered by an Iota One controller (from General Valve). A delay of 600 μ s between nozzle opening and the laser firing was introduced using a delay/pulse generator (Stanford Research Systems, model DG535). The nozzle diameter was 0.5 mm. The laser intersected the molecular beam 0.5-1.0 cm downstream in all experiments.

Fluorescence was collected at a right angle using a Hamamatsu R928 photomultiplier tube cooled to -25 °C. The output was amplified and gated for 100 μ s with Evans Associates circuitry. To improve signal

collection, a spherical mirror (diameter = 60.0 mm, focal length = 25.0 mm) was placed opposite the photomultiplier tube (PMT), on the other side of the molecular beam. Fluorescence was focused on the PMT by means of two lenses (diameter = 50.8 mm, focal length₁ = 50.8 mm, and focal length₂ = 101.6 mm). For one photon excitation a diaphragm and a 2 mm thick WG-320 filter were used to reduce background noise. It was

TABLE 1. Temperatures used in the Jet Experiments.

Molecule or Complex	Sample Container Temperature (°C)	Jet Nozzle Temperature (°C)
Bare Indole	50	60
Indole-Water	50-70	60-75
Indole-Methanol	60	75
Indole-Formamide	60-65	75
Bare 3-Methylindole	50-80	60-95
3-Methylindole-Water	55-95	65-115
3-Methylindole-Methanol	85	105
3-Methylindole-Ethanol	85	105
3-Methylindole-Butanol	85	105
3-Methylindole-Diethylether	85	105
3-Methylindole-Diethylamine	85	105
3-Methylindole-Triethylamine	85	95-105
Bare 2,3-Dimethylindole	75-95	105-110
2,3-Dimethylindole-Water	80-95	95-110
7-Azaindole	75	95
7-Azaindole-Water	75-105	95-115

eventually found that, with careful laser alignment, either no filter or a diaphragm with a saturated aqueous solution of NiSO₄ (1 cm path length), gave superior signal-to-noise. For two photon excitation a 3 mm

thick UG-11 filter and a saturated aqueous solution of NiSO_4 (1cm path length) were used to reduce background noise. In the dispersed fluorescence experiment the emission was collected at a right angle through the same two-lens system and focused into a 2 mm (core diameter) UV transmitting plastic clad fiber optic (Fiberguide Industries). The light was carried about 3.3 m by the fiber and focused using an $f/7$ optical system into a Spex 1404 double spectrometer with a 2400 g/mm grating (linear dispersion = 0.2nm/mm), where the dispersed emission was measured using a Hamamatsu R928 photomultiplier tube cooled to -25°C . Slit widths varied with the desired resolution. The monochromator resolution is reported in the figures as twice the spectral bandpass (full width at half maximum). In all experiments, signals were normalized by dividing the signal by the laser energy (or the square of the laser energy when measuring the two-photon signal) measured with a homemade quantum counter previously described(53).

Calculations

Computer Hardware

Calculations necessary for spectral simulations were performed on a Zeos Meridian 400 subnotebook computer with an Intel 486 100 MHz processor and 8 MB of RAM.

Computer Software

Programs used in the spectral simulations were originally written in Fortran by Patrik Callis. They were modified somewhat before use in this work.

Spectral Simulations

Simulation of dispersed fluorescence spectra used a procedure similar to that described previously(32). The method is shown schematically in Figure 7.

Briefly, the spectra were constructed by first converting the bare indole or the bare 3-methylindole dispersed fluorescence spectrum to a stick spectrum of the intensities. A stick spectrum was then constructed from the group of peaks starting near 765 cm^{-1} in both the indole-water and indole-methanol dispersed fluorescence spectra, and at the origin in the 3-methylindole-water dispersed fluorescence spectrum. For indole

Method of Spectral Simulation

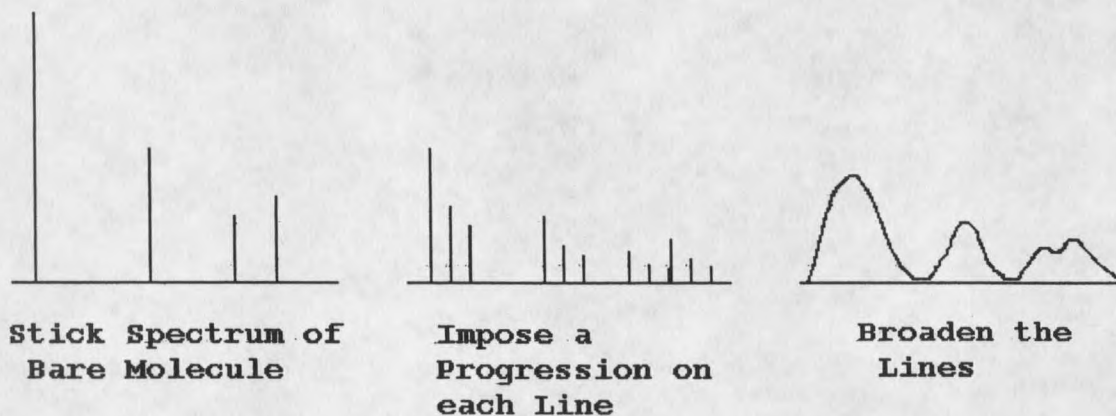


Figure 7. The method used in simulating spectra is shown.

water the intensities at 767, 783, 792.1, 805.8, 821.8, 836.6, 851.4, 861.6, and 877.5 cm^{-1} were used. For indole-methanol the intensities at 764, 805, 844.8, 887.9, 935.4, and 974.9 cm^{-1} were used. For 3-methylindole the intensities at 0.0, 22.5, 45, 74.5, 98, 119.2, 135.7, 159.2, 179.1, 210.8, 234.2, 252.8, 276.2, 294.8, 330.9, and 354.1 cm^{-1} were used. These stick spectra from the complexes were substituted for each line of the bare indole stick spectrum and normalized to contain

the same total intensity as the line being replaced. The resulting stick spectra were then broadened with a Gaussian until a close match with experimental dispersed fluorescence spectra was obtained.

RESULTS AND DISCUSSION

Indole-Polar Solvent ComplexesIndole-Water

Figure 8 shows the one-photon fluorescence excitation spectrum of the indole-water complex. The origin regions of the σ - and ρ -complexes, of the bare indole molecule are shown.

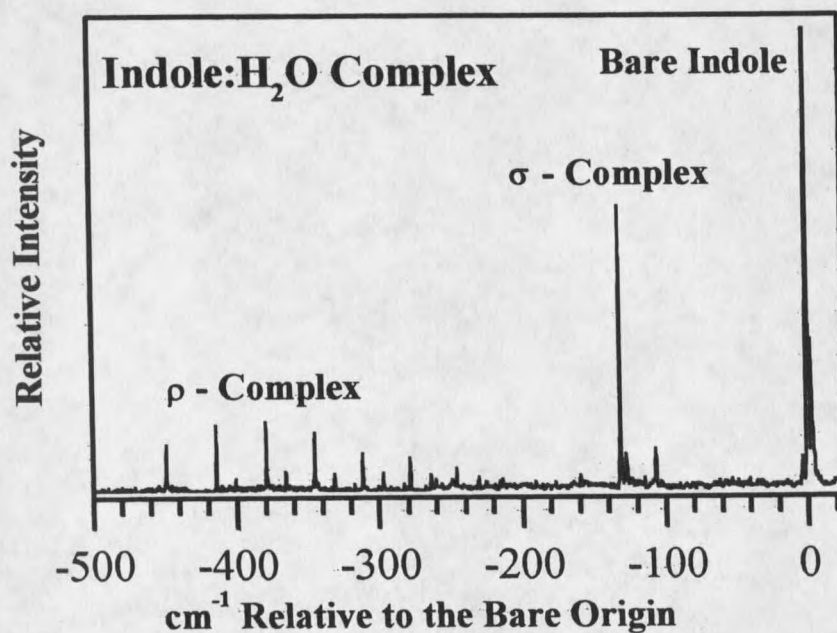
Fluorescence Excitation

Figure 8. The fluorescence excitation spectrum of the origin regions of the indole-water ρ - and σ -complexes and of bare indole is shown.

The shifts from the bare indole origin are -132 and -450 cm^{-1} , for the σ - and ρ -complexes, respectively. Polarized two-photon excitation spectra for the first four peaks, starting at -450 cm^{-1} , of the 35 cm^{-1}

progression of the ρ -complex are shown in Figure 9a-d.

Indole-Water Two-Photon Excitation

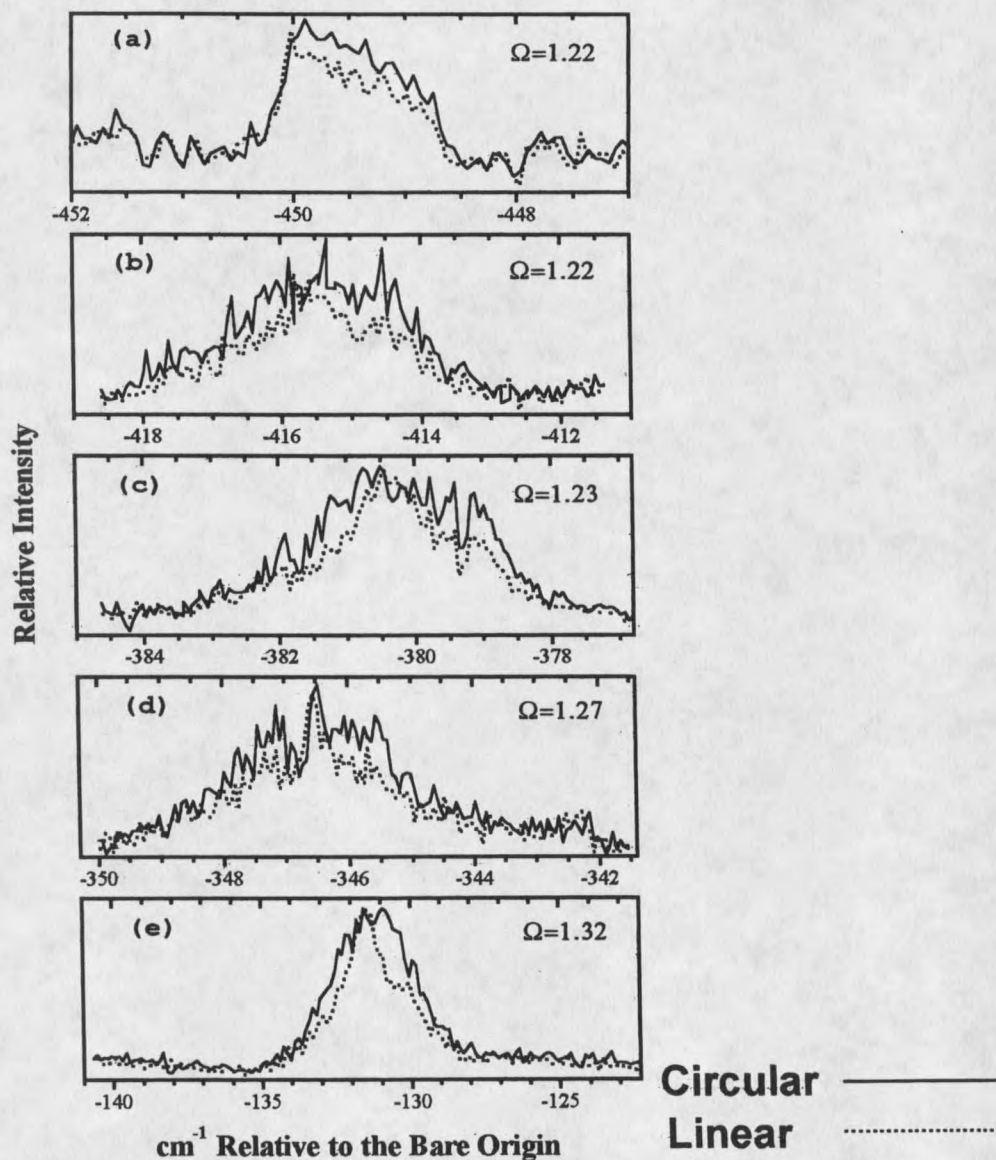


Figure 9. Polarized two-photon excitation spectra are shown. (a)-(d) the ρ -complex. (e) the σ -complex.

The Ω -values of 1.2 to 1.3 show that excitation is to the 1L_b state and that this state is the lowest excited state for the ρ -complex. Since the individual complexes are isolated from one another in the jet, this is the state from which emission is expected to occur. The two-photon spectrum of the σ -complex, which is known to have 1L_b emission(29), is shown for comparison [Figure 9e].

The high-resolution dispersed fluorescence spectrum of the indole-water ρ -complex is shown in Figure 10b. It does not have the broad redshifted component present in a low-resolution spectrum of the same complex(see reference 29). This spectrum has two regions in which well-resolved progressions are visible. These start at the origin and near 760 cm^{-1} to the red of the excitation. Scans with only the laser on and the pulsed valve of the jet off show that most of the intensity at the origin is due to scattered light.

There are two characteristics of the indole-water dispersed fluorescence spectrum (Figure 10b) that were unexpected. First, the progressions in the ground state(Figure 11a) did not have the evenly spaced lines found in the excited state(Figure 8). Lower resolution spectra, like that in Figure 10b, had suggested a progression with the second peak at 17 cm^{-1} and a $14\text{-}15\text{ cm}^{-1}$ spacing of subsequent peaks. When higher resolution spectra were collected this characterization broke down. A tentative assignment of the vibronic structure based on a minimum number of vibrations was made. It is found that this spectrum can be characterized by five active vibrations (see Table 2). Some lines have more than one possible assignment, because different combinations were found to fit the same frequency. One caveat needs to be stated about this assignment. It is somewhat unexpected that certain modes, particularly $2\nu_1$ and $\nu_1\nu_2$, are absent. The possibility can not be ignored

Dispersed Fluorescence Indole-Water

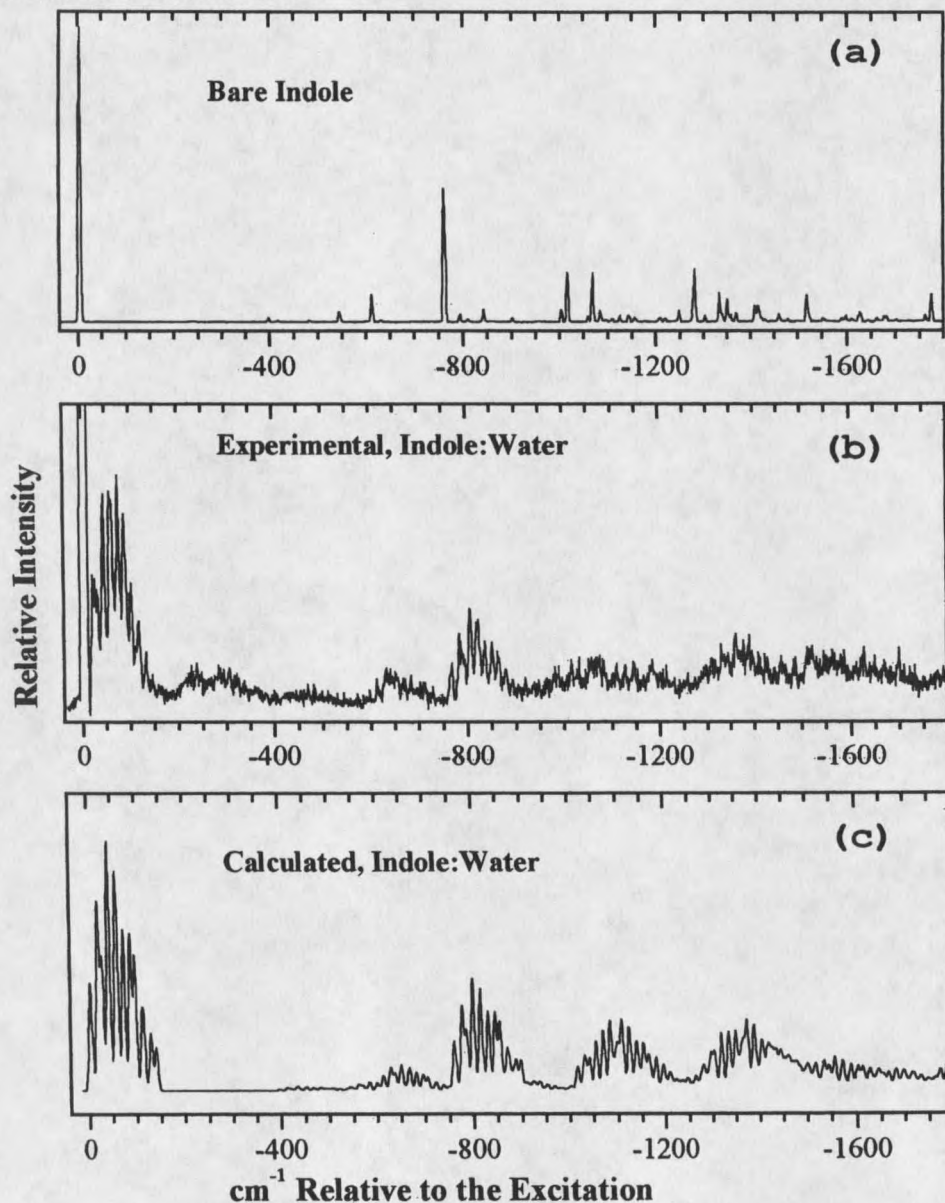


Figure 10. Dispersed fluorescence spectra (excitation at the origins) are shown for (a) bare indole, (b) the indole-water ρ -complex, and (c) the simulated spectrum for the indole-water ρ -complex. The monochromator resolution for the bare indole spectrum is about 7 cm⁻¹ and for the experimental indole-water spectrum about 14 cm⁻¹.

that this spectrum actually is a progression of one vibrational mode, which has been somewhat distorted by the local structure of the 1:2, indole:water, complex.

It is noted that there are more lines listed in Table 2 than are present in Figure 11a. The reason is that if the excitation is to higher levels of a given vibrational mode of the excited state, the wave functions of those levels have a different overlap with the ground state manifold. This is illustrated in Figure 11a-d, where excitation is to the first, second, third, and fourth lines of the most intense excited state progression of the ρ -complex. That these lines belong to the same vibrational mode is shown by the fact that the number of nodes increases from zero to three from the first to fourth line of the progression.

The second unusual characteristic of the indole-water dispersed fluorescence spectrum (Figure 10b) is the emission between 200 and 400 cm^{-1} , that was not expected when considering the spectrum of bare indole (Figure 10a). The intensity between 200 and 400 cm^{-1} was shown to be from the ρ -complex, by setting the monochromator in this region and scanning the excitation with the laser. For monochromator settings of 200, 280, 300, 325, 350 and 400 cm^{-1} to the red of the complex origin the resulting spectra all closely resembled that of the ρ -complex shown in Figure 8. The fluorescence excitation spectra detected at 200, 300, and 400 cm^{-1} to the red of the complex origin are shown in Figure 12. The presence of the ρ -complex origin transition at -450 cm^{-1} in each of these excitation spectra proves that the dispersed fluorescence in the 200 to 400 cm^{-1} region is from the ρ -complex. It is not known why fluorescence intensity is present in this region, but one guess is the following. In a study from the Zwier group(40) in which it was shown that the ρ -complex is a

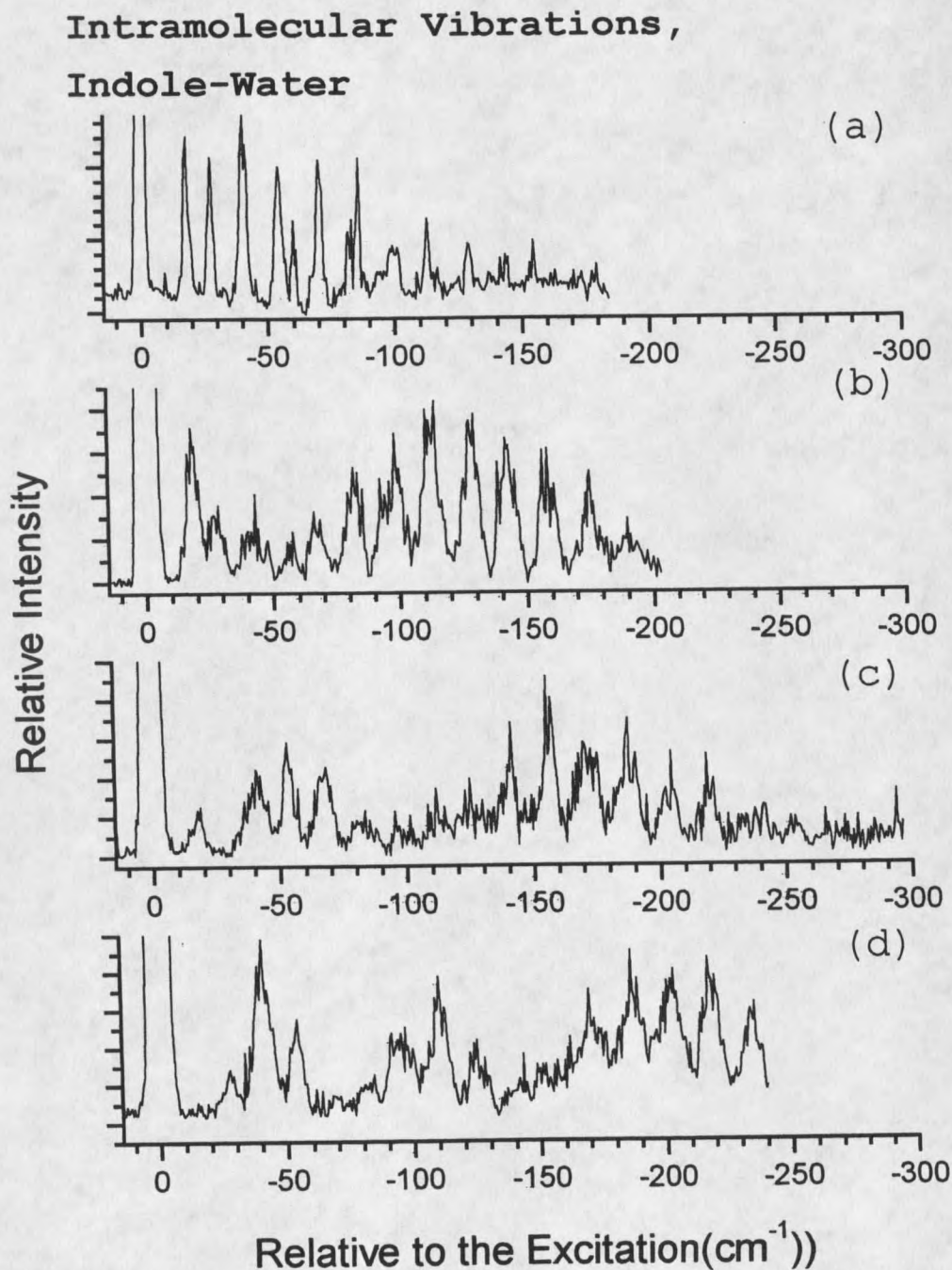


Figure 11. Dispersed fluorescence spectra of the Indole-Water ρ -complex are shown, with excitation at (a) the ρ -complex origin, (b) the ρ -complex origin $+35.2 \text{ cm}^{-1}(\nu_1)$ (52), (c) the ρ -complex origin $+69.9 \text{ cm}^{-1}(2\nu_1)$, and (d) the ρ -complex origin $+103.9 \text{ cm}^{-1}(3\nu_1)$. The monochromator resolution is about 3 cm^{-1} in (a) and about 9 cm^{-1} in (b)-(d).

Table 2. Tentative Assignment of the Intramolecular Indole-Water Vibrations (see Figure 11)

Red Shift from the Origin (cm^{-1})	Peak Assignment
17.7	ν_1
27.1	ν_2
40.0	ν_3
54.2	$2\nu_2$
60.0	$\nu_1\nu_3$
70.0	ν_4
81-82	$3\nu_2$
85.9	ν_5
98-101	$\nu_12\nu_3, \nu_13\nu_2$
110-112	$\nu_3\nu_4, \nu_12\nu_2\nu_3$
128.6	$\nu_3\nu_5, \nu_1\nu_3\nu_4$
142-144	$\nu_1\nu_3\nu_5$
154-158	$\nu_4\nu_5, \nu_12\nu_4$
169-175	$2\nu_5, 2\nu_12\nu_22\nu_3, \nu_1\nu_4\nu_5$
186-188	$\nu_12\nu_5, \nu_24\nu_3$
202-205	$2\nu_12\nu_5, \nu_1\nu_22\nu_4$
217-219	$2\nu_32\nu_4, \nu_1\nu_22\nu_5$
235-236	$2\nu_1\nu_22\nu_5$

1:2, indole:water, complex, there are unexplained sidebands on at least two of the peaks of the resonant ion-dip infrared spectrum. We have suggested, and the Zwier group has agreed (see their note under reference 20 of (40)), that these may represent a second 1:2, indole:water, complex. This would assume that the 1:2 complexes are indistinguishable from each other in their one-color resonant two-photon ionization spectrum (it gives the same information as the fluorescence excitation spectrum in Figure 8), since they observed only one set of peaks for the 1:2 complex (Figure 1 of reference (40)). It is also interesting to note that they have found (as have we, David Hahn - unpublished results) in *ab initio* calculations two stable forms of the 1:2 complex separated in energy by only 0.7 kcal/mole (244.8 cm^{-1}). We suggest that the

Fluorescence Excitation, Indole-Water Specific Detection

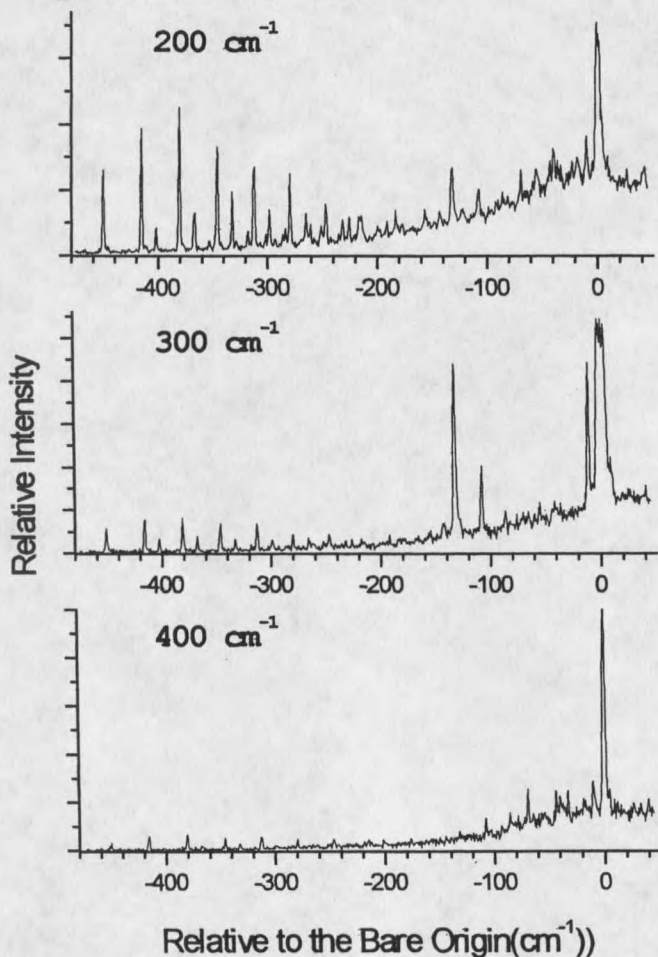


Figure 12. Fluorescence excitation spectra of the indole-water ρ -complex detected at 200, 300, and 400 cm^{-1} to the red of the complex origin are shown. The monochromator window was 140 cm^{-1} for detection at 200 cm^{-1} , and 47 cm^{-1} for detection at 300 and 400 cm^{-1} .

unexpected emission in the -200 to -400 cm^{-1} region of our indole-water spectrum may be due to a second stable form of the 1:2, indole:water, complex.

Indole-Methanol

In Figure 13 the one-photon fluorescence excitation spectrum of the

indole-methanol complex is shown. Again, the origin regions of the ρ -complex, the σ -complex, and of bare indole are shown. The shifts from the bare origin are -160 and -469 cm^{-1} for the σ - and ρ -complexes, respectively. The splitting of the origin region for the ρ -complex is not a regular progression as is observed for the indole-water ρ -complex.

Two-photon fluorescence excitation spectra of the first three major peaks of the ρ -complex are shown in Figures 14a-c. The Ω -values of 1.13 to 1.26 show that excitation is to the 1L_b state. Also shown is the two-photon excitation spectrum for the indole-methanol σ -complex [Figure 14d]. The Ω -value of 1.35 is characteristic of excitation to the 1L_b state.

Fluorescence Excitation

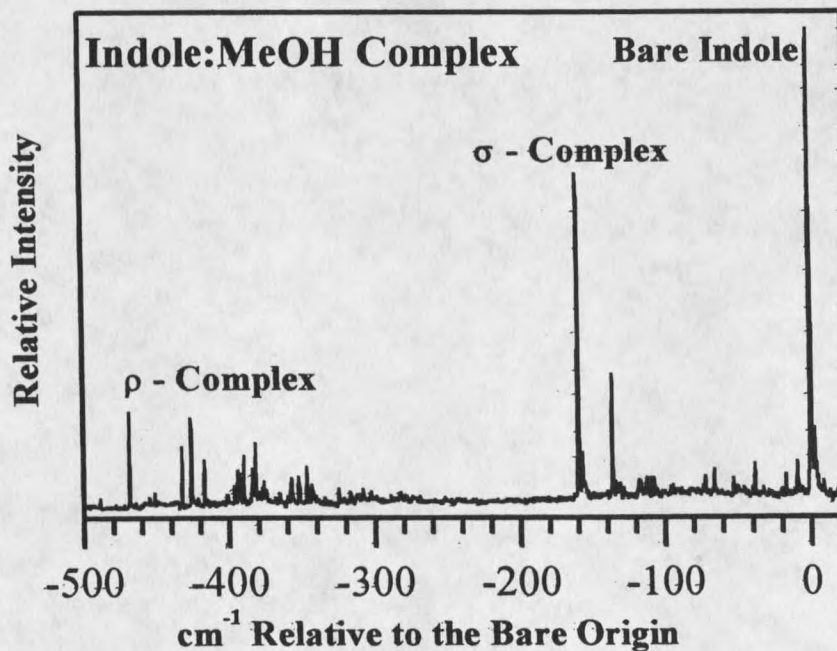


Figure 13. The fluorescence excitation spectrum of the origin regions of the indole-methanol ρ and σ -complexes and of bare indole is shown.

Indole-Methanol Two-Photon Excitation

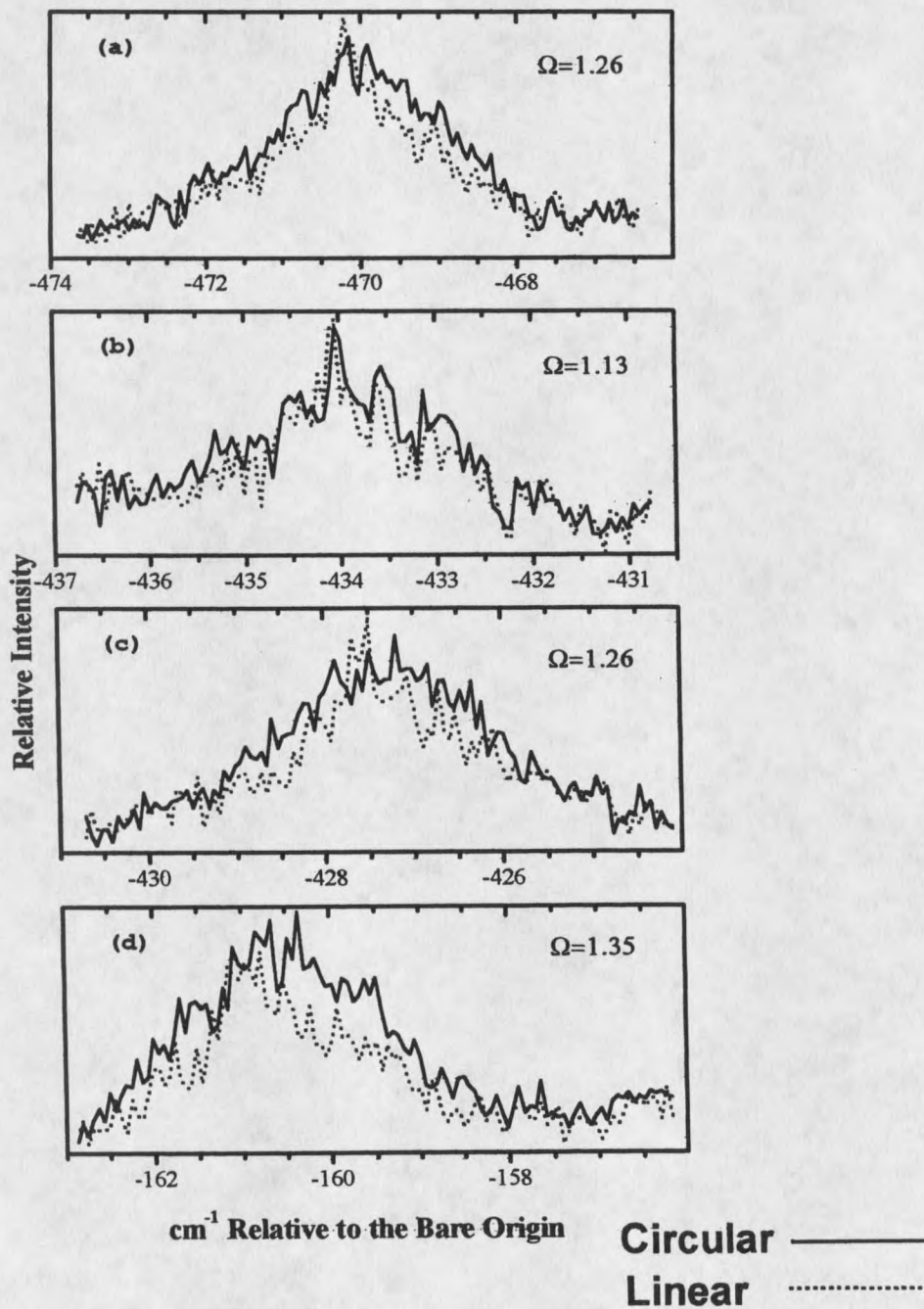


Figure 14. Polarized two-photon excitation spectra are shown. (a)-(d) the ρ -complex. (e) the σ -complex.

Indole-Methanol Dispersed Fluorescence

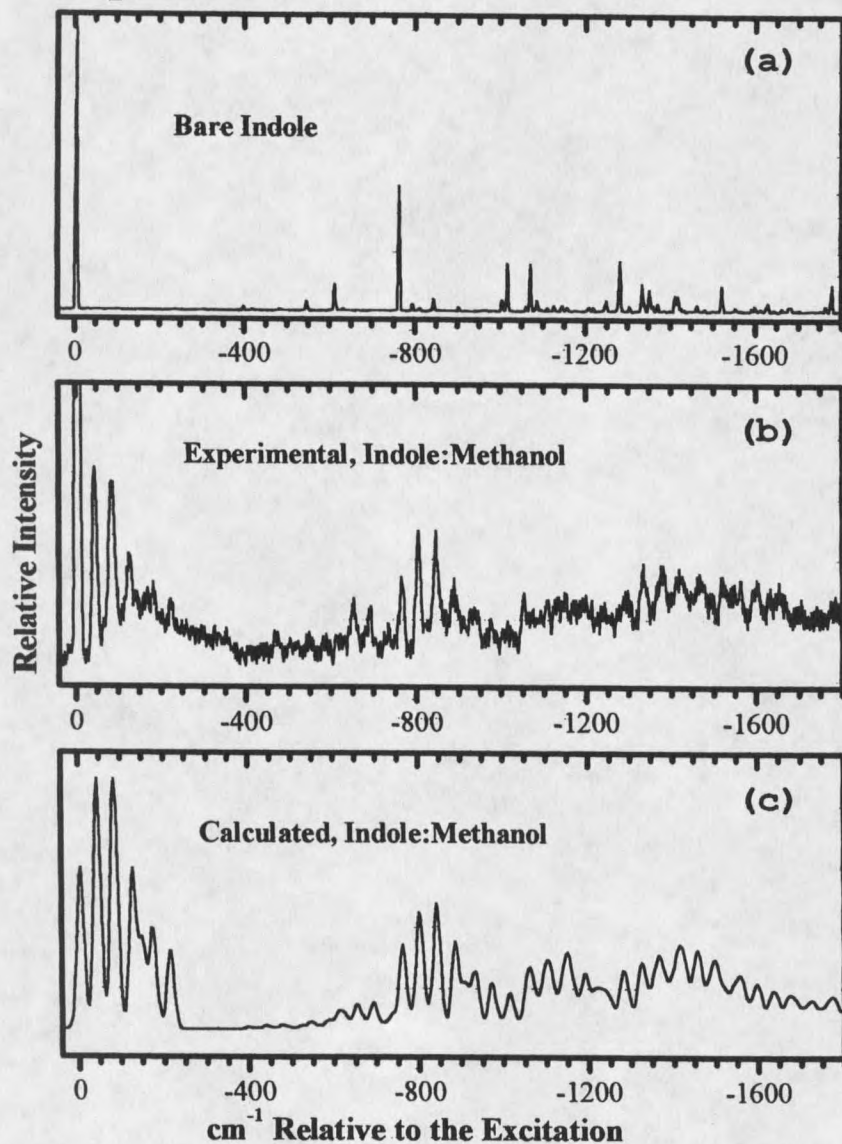


Figure 15. Dispersed fluorescence spectra are shown for (a) bare indole, (b) the indole-methanol ρ -complex, and (c) the simulated spectrum for the indole-methanol ρ -complex. The monochromator resolution for the bare indole spectrum is about 7 cm^{-1} and for the experimental indole-methanol spectrum about 19 cm^{-1} .

Figure 15 shows a high-resolution dispersed fluorescence spectrum of

the indole-methanol ρ -complex. The regions near the origin and near 650, 760, and 1330 cm^{-1} show groups of well-resolved peaks. It is noted that, like the indole:water spectrum in Figure 10b, the indole:methanol spectrum in Figure 15b displays intensity between -250 and -400 cm^{-1} that can not be duplicated in the calculated spectrum in Figure 15c.

In dispersed fluorescence spectra, much of the intensity at the excitation energy is due to scattered light. An estimate of the scattered component can be obtained by taking the difference between the signal with the pulsed valve of the jet on and with it off. This

**Indole-Methanol
Dispersed Fluorescence
Difference Spectrum**

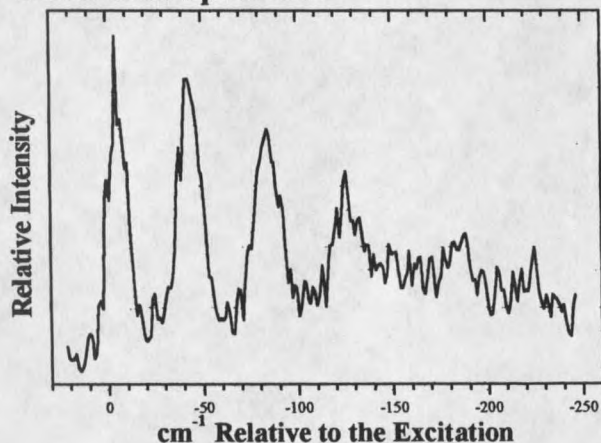


Figure 16. The difference spectrum for the indole-methanol origin region is shown. The signal with the supersonic jet pulsed valve off is subtracted from the signal with it on. The monochromator resolution is about 19 cm^{-1} .

difference for the origin region of the indole-methanol ρ -complex is shown in Figure 16. With the scattered light subtracted out, the peak structure in the origin region now more closely resembles that in the region starting near 760 cm^{-1} (see Figure 15a). This is important, because intensities of the peaks near 760 cm^{-1} are used to simulate the

entire spectrum.

Indole-Formamide

Formation of the indole-formamide complex was first verified by comparison of the one-photon fluorescence excitation spectrum (Figure 17a) with that published previously(29). Figure 17c shows the polarized two-photon fluorescence excitation spectrum of the lowest energy peak of the complex. An Ω -value of 1.46 leaves little doubt that excitation is to the 1L_b state. A high-resolution dispersed fluorescence spectrum from this peak, is shown in Figure 17b. The regions near the origin and starting near 760 cm^{-1} show groups of well-resolved peaks.

Simulation of Spectra

Simulated spectra for the indole-water and indole-methanol complexes are shown in Figures 10c and 15c, respectively. It has been noted before(32) that the dispersed fluorescence spectrum of the indole-water complex, found by Tubergen and Levy(29) and identified as 1L_a fluorescence, could be plausibly simulated without reference to the 1L_a state. This was done by taking the bare molecule 1L_b spectrum of Bickel et al.(13) and substituting the 35 cm^{-1} progression from the excitation spectrum for each vibronic line(32). The resulting spectrum was then broadened by 50 cm^{-1} . We have improved the simulation method by using the bare molecule stick spectrum from our own dispersed fluorescence data (Figures 10a or 15a), and imposing on it the low-frequency Franck-Condon pattern found in the dispersed fluorescence spectra of the complexes (Figure 10b and Figure 15b). After broadening, the resulting spectra (Figure 10c and Figure 15c) are found to match experimental data remarkably well. The main difference between the observed and simulated spectra is the absence of the unanticipated bands in the $200\text{-}400\text{ cm}^{-1}$

Indole-Formamide

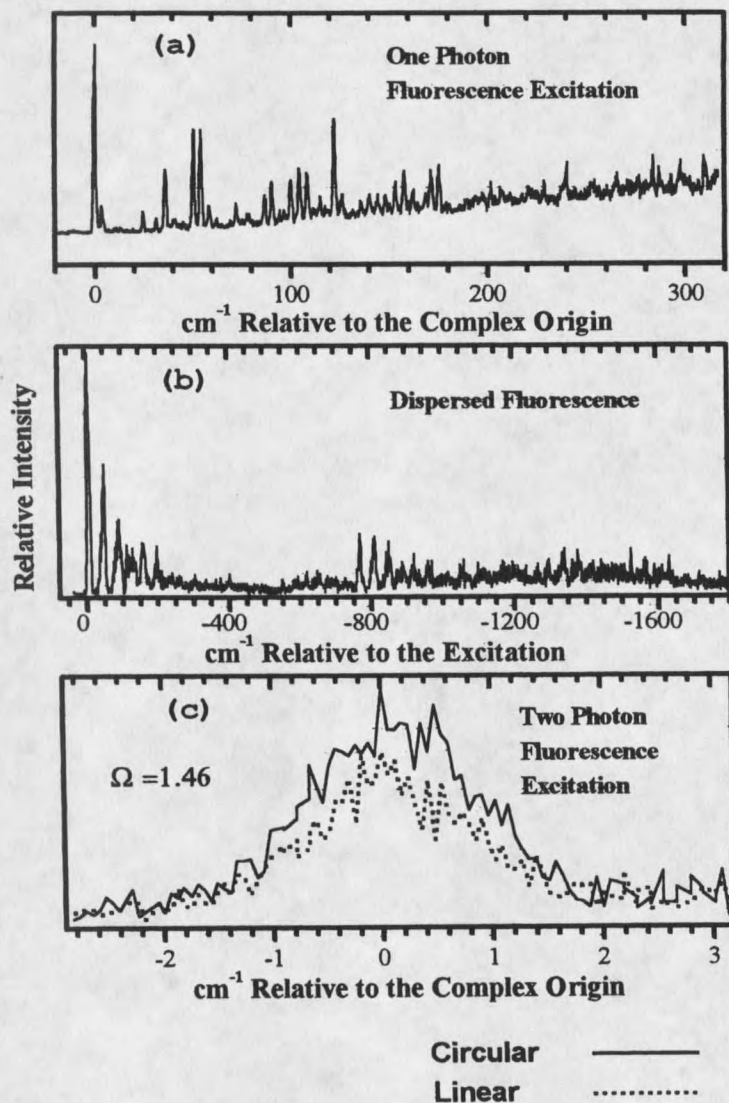


Figure 17. Spectra for the 1:1, indole-formamide are shown. They are (a) one-photon fluorescence excitation, (b) two-photon fluorescence excitation of the complex origin, and (c) dispersed fluorescence from the complex origin. The monochromator resolution in (c) is about 14cm^{-1} .

region, that are not observed in the fluorescence from bare indole. There is also no evidence of them in the excitation spectrum of the ρ -complexes. The missing intensity is probably the reason for the small

amount of intensity missing from the gaps at about 900 and 1200 cm^{-1} in the simulated spectra. This is because monitoring the intensity in the 200-400 cm^{-1} region gives the same excitation spectrum as when monitoring the entire spectrum, so this intensity is expected to be a satellite of all bands in the spectrum. As stated above, this intensity is likely connected to multiple conformations of the 1:2, indole:water, complex and so can not be attributed to 1L_a emission. Since the spectra of the ρ -complexes can be simulated by starting with the bare molecule 1L_b spectrum and imposing on it the Franck-Condon pattern from the low frequency intermolecular modes, it is likely that emission in the complexes is from the 1L_b state.

Origin of Broad Redshifted Emission

In previously reported investigations of the indole-polar solvent complexes studied here, the broad redshifted fluorescence found was taken as a sign of emission from the 1L_a state (28,29,36). The redshifted component is likely due to an increased density of lines in combination with instrumental broadening. It is useful to consider an example of how this can occur. Figure 18 shows a comparison of two simulated spectra of the indole-water ρ -complex.

The two spectra differ only by the width of the Gaussian broadening given to the lines, 1 or 100 cm^{-1} (FWHM - full width at half maximum). The spectrum with 1 cm^{-1} broadening (Figure 18a) has low relative intensity in the region above 2000 cm^{-1} . The spectrum with 100 cm^{-1} broadening (Figure 18b) however, has a higher relative intensity in this region. And, although the first moments in the two spectra are identical, that of the lower resolution spectrum appears to be redshifted from that of the spectrum with 1 cm^{-1} resolution. These two things occur because the large number of weak, closely spaced lines

Indole-Water Simulated Spectra

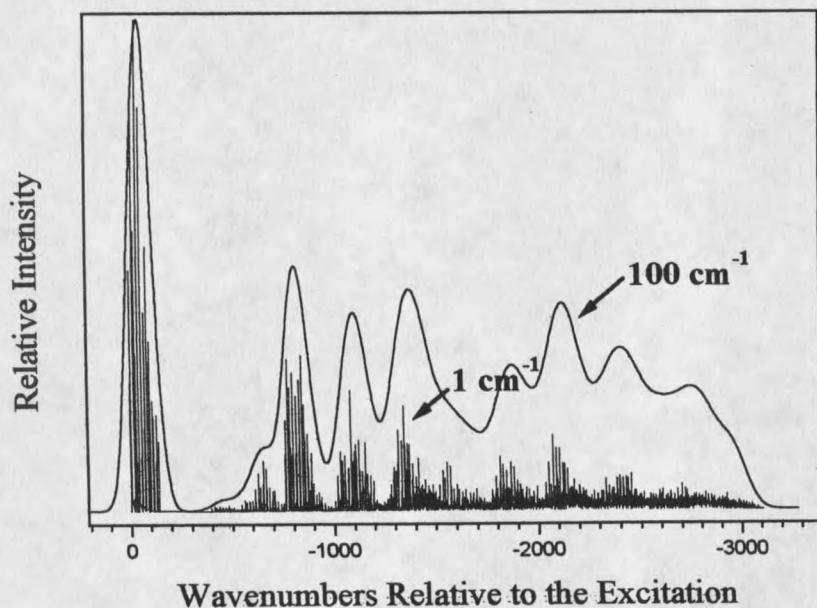


Figure 18. A comparison of two indole-water simulated spectra are shown. They are broadened to 1 and 100 cm^{-1} (full width at half maximum) respectively.

coalesce into peaks when the spectra are broadened. It is thus apparent that care must be taken in identifying the emitting state of low resolution spectra.

Consideration of Exciplexes

It has been suggested(29) that the two different complexes formed by indole with polar solvents are the same as the exciplexes(38) that have been postulated to explain the fluorescence of indole and 3-methylindole in room temperature hydrocarbon solutions containing minute amounts of various alcohols. There are several reasons why this is unlikely. First, the jet-cooled spectra are for ground state complexes, whereas the exciplexes are believed to form only in the excited state. Second, the

two exciplexes were both postulated as π -complexes, which does not explain the occurrence of the σ -complex. Finally, the recent evidence(40) concerning the stoichiometry (1:2, indole:water) and geometry of the indole-water ρ -complex suggests that assignment as a 1:1 alcohol π -complex may be incorrect.

Summary of the Evidence of 1L_b Emission

Two points supporting 1L_b emission in the indole-polar solvent complexes have been covered above. First, since excitation is to the 1L_b state, the emission in a jet environment is expected to be from that state. Second, the dispersed fluorescence spectra of the complexes can be simulated by starting with 1L_b emission from the bare molecule, imposing the intermolecular vibrational progression on each line of that spectrum, and broadening the result with a Gaussian function.

There are also specific spectral characteristics that can be used to distinguish 1L_a and 1L_b emission. In bare indole the most Franck-Condon active vibration is ν_{26} , with a frequency of 760 cm^{-1} in the ground state(54). For bare indole in the jet (see Figures 10a and 15a), its intensity is close to 50% of the origin intensity. In the indole-water, indole-methanol, and indole-formamide complexes (see Figures 10b, 15b, and 17c) this intensity is also approximately 50%. In addition, the ν_{27} (610 cm^{-1}) activity is much weaker and there is little or no evident Franck-Condon activity of the C-C stretching modes that would appear near 1600 cm^{-1} . This pattern has been well reproduced by geometry changes and normal modes obtained for the 1L_b transition from *ab initio* calculations(41). The same calculations give considerably different Franck-Condon factors for the 1L_a transition, and produce spectra in good agreement with 1L_a fluorescence from 2,3-dimethylindole(42) and 3L_a

phosphorescence (9,54) from indole in argon matrices at 20 K. Also, recent calculations in our lab on the 1:2, indole:water, complex (David Hahn - unpublished results), predict that although the 1L_a state has a larger redshift than the 1L_b state, it is not large enough to invert the states. These theoretical predictions, and the absence of the characteristics of 1L_a Franck-Condon activity in the dispersed fluorescence spectra of the three complexes means that the emission is from the 1L_b state.

3-Methylindole-Polar Solvent Complexes

Fluorescence Excitation

Figure 19 shows the one-photon fluorescence excitation spectra of the various 3-methylindole polar solvent complexes. A number of these have been reported previously (15,34,36). It is noted that, unlike indole, only one solvent complex is observed for 3-methylindole complexed with water and methanol (34,36). The red-shifts of the complex origins from the bare origin are 233.8 cm^{-1} for water, 288.3 cm^{-1} for methanol, 385.8 cm^{-1} for ethanol, 385.5 cm^{-1} for butanol, 428.5 cm^{-1} for diethyl ether, 709.8 cm^{-1} for diethylamine, and 676.5 cm^{-1} for triethylamine. It is assumed, although not proven, that all the complexes involve formation of a hydrogen bond to the nitrogen proton on the pyrrole ring of 3-methylindole (34).

There are a couple of interesting things to note about the spectra in Figure 19. First, it is possible to assign vibrational progressions for the butanol, diethylether, diethylamine, and triethylamine complexes, that have not previously been assigned. They are listed in Table 3.

Table 3. Assignment of Progressions for the 3-Methylindole Complexes

Complexing Solvent	Peak Positions (cm^{-1})
Butanol	19-20, 81, 140
Diethylether	0, 76.1, 151.9, 228.7
Diethylether	212.5, 290.4, 367.5
Diethylether	238, 326.4, 409
Diethylamine	0, 84.5, 167.7, 249.8
Triethylamine	0, 106.2, 212.9 (see arrows on figure)
Triethylamine	80.9, 171.9, 260.4
Triethylamine	100.6, 185.8, 268-270

The second interesting thing to note is the apparent vibrational structure of the 3-methylindole-triethylamine spectrum. With the exception of the butanol complex, the origin band is the largest vibronic band in the spectra of the other 3-methylindole-polar solvent complexes. For triethylamine it is somewhat smaller than the 80.9 cm^{-1} peak. Also, it was noticed that the diethylamine complex has a very small peak at -25.9 cm^{-1} relative to its assigned origin (see the arrow in the 3-methylindole-diethylamine spectrum in Figure 19). This suggests the possibility that the real origin for the 1:1 3-methylindole-triethylamine complex might be at 80.9 cm^{-1} , and that the peak at 0 cm^{-1} might represent a complex with more than one triethylamine molecule. There is however a reason why the origin assignment might be correct. It is possible to assign at least three progressions in the $0-300 \text{ cm}^{-1}$ region of this spectrum (see Table 3). Triethylamine is somewhat larger than the other complexing solvents, and so it may form more than one stable 1:1 complex with 3-methylindole. So it is possible the peaks at 0 , 80.9 , and 100.6 cm^{-1} could represent multiple 1:1 complexes.

Fluorescence Excitation 3-Methylindole Complexes

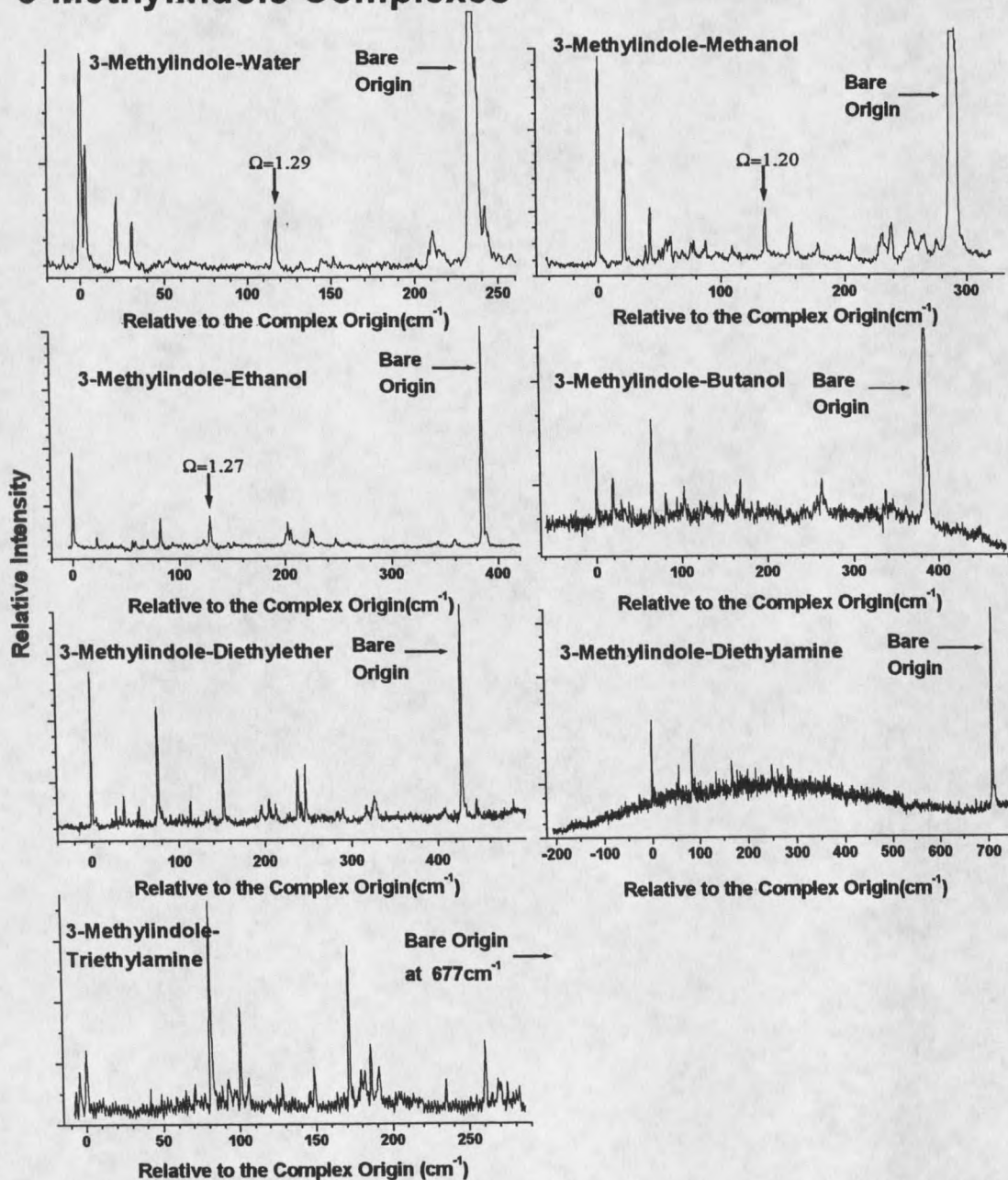


Figure 19. Fluorescence excitation of 3-methylindole-polar solvent complexes are shown. The position of the bare 3-methylindole origin is labeled in each spectrum. The Ω -values of several peaks are labeled.

Two-Photon Excitation

In Figure 20 are shown polarized two photon excitation spectra for the origin peaks of bare 3-methylindole and of each of the van der Waals complexes. For bare 3-methylindole the Ω -value of 1.23 suggests that excitation is to the 1L_b state. The Ω -values of the complexes progressively decrease from 0.99 to about 0.55 as the proton affinity of the solvent increases (see Table 4). This suggests that the 1L_a character of the state to which the complex is excited increases as the proton affinity of the solvent increases. The diethylamine and triethylamine spectra appear to have an underlying background for excitation with linearly polarized light. The cause of this is unclear, but it is possible it represents underlying emission from clusters with more than one solvent molecule.

Dispersed Fluorescence

High-resolution dispersed fluorescence spectra of bare 3-methylindole and of each of the complexes are shown in Figure 21. In each case excitation is at the origin peak of the bare molecule or respective complex. Bare 3-methylindole shows characteristics expected of emission from the 1L_b state. The spectra of the complexes also show some of the characteristics expected of 1L_b emission along with varying degrees of the characteristics expected with 1L_a fluorescence. As the discussion below will show, the 1L_a character of the emitting state increases with increasing proton affinity of the complexing solvent.

Figure 22 shows a comparison of the dispersed fluorescence spectra of bare 3-methylindole and the 3-methylindole-water complex. The spectra have been scaled so that the origin peak at 0 cm^{-1} has the same height in both. Each peak in the spectrum of the complex has a series

Polarized Two-Photon Excitation 3-Methylindole Complexes

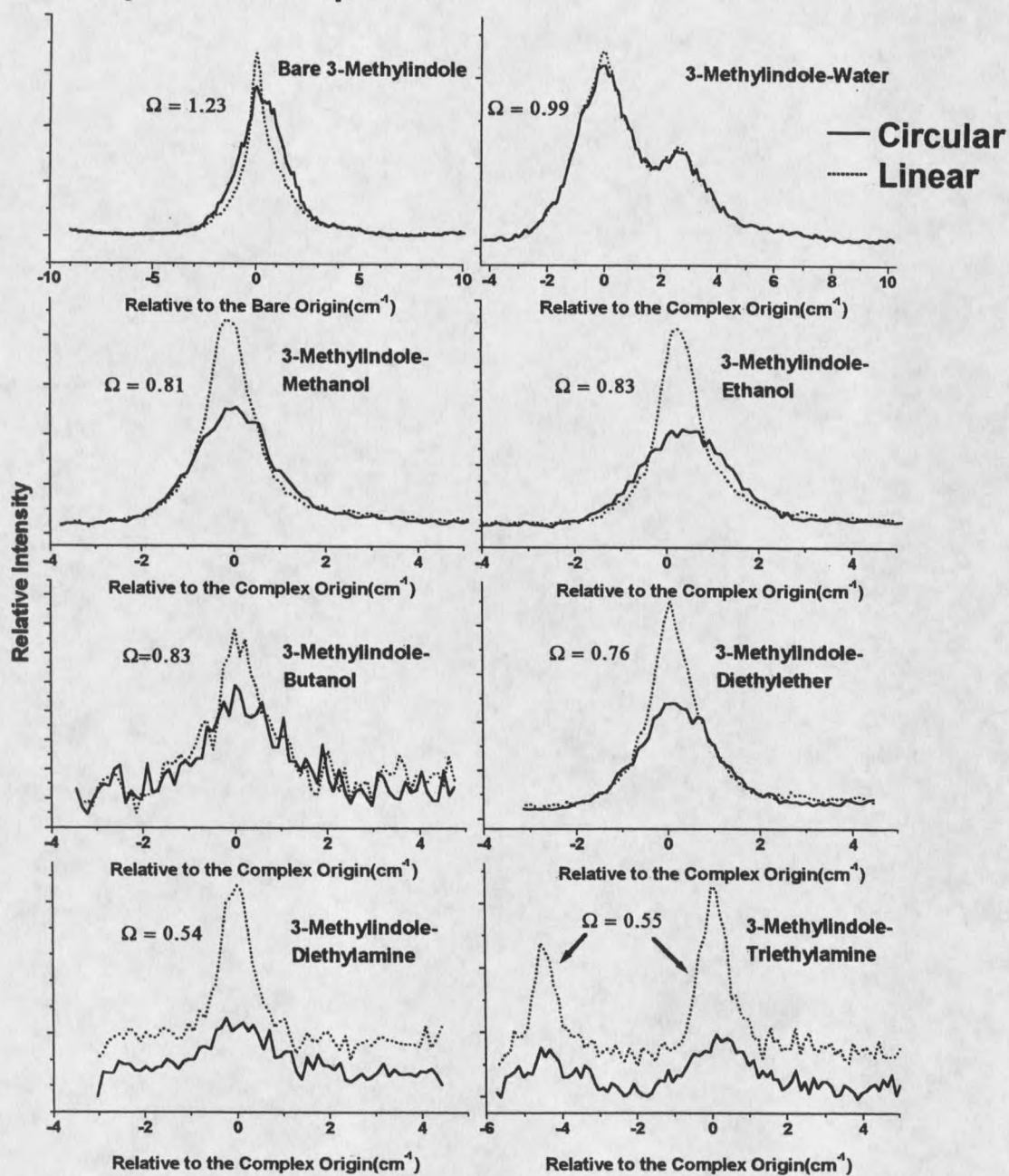


Figure 20. Polarized two-photon excitation spectra of bare 3-methylindole and the polar solvent complexes are shown. Ω -values are given in each spectrum.

Table 4. 3-Methylindole Complexes, Proton Affinities and Ω -Values

Complexing Solvent	Proton Affinity	Origin Ω -Value
Water	166.5	0.99
Methanol	181.9	0.81
Ethanol	188.3	0.83
Butanol	195*	0.83
Diethyl Ether	200.2	0.76
Diethylamine	225.1	0.54
Triethylamine	231.2	0.55

*Estimated

of peaks built off of it due to the intermolecular vibrational modes between 3-methylindole and water. This is particularly noticeable for the origin peak. There are also apparent changes in the intensity of peaks of the complex that should be noted. Peaks at 708, 760, 1129, and 1355 cm^{-1} all show increased intensity in the complex relative to the bare molecule. In the 1500-1700 cm^{-1} region there is increased intensity in the complex, and there is the appearance of at least one new peak. As considered below, emission in this region is characteristic of that expected from the 1L_a state.

Further Characterization of the Higher Vibronic Levels of the Water, Methanol, Ethanol, and Triethylamine Complexes

In an attempt to gain a better understanding of changes in the relative locations of the 1L_a and 1L_b states when 3-methylindole forms complexes with polar solvents, additional polarized two-photon excitation spectra were collected of the higher vibronic levels of four of the complexes. Spectra for the 3-methylindole complexes with water, methanol, ethanol, and triethylamine are shown in Figures 23, 24, 25, and 26.

Dispersed Fluorescence, 3-Methylindole Complexes

(Excitation at the Complex Origin)

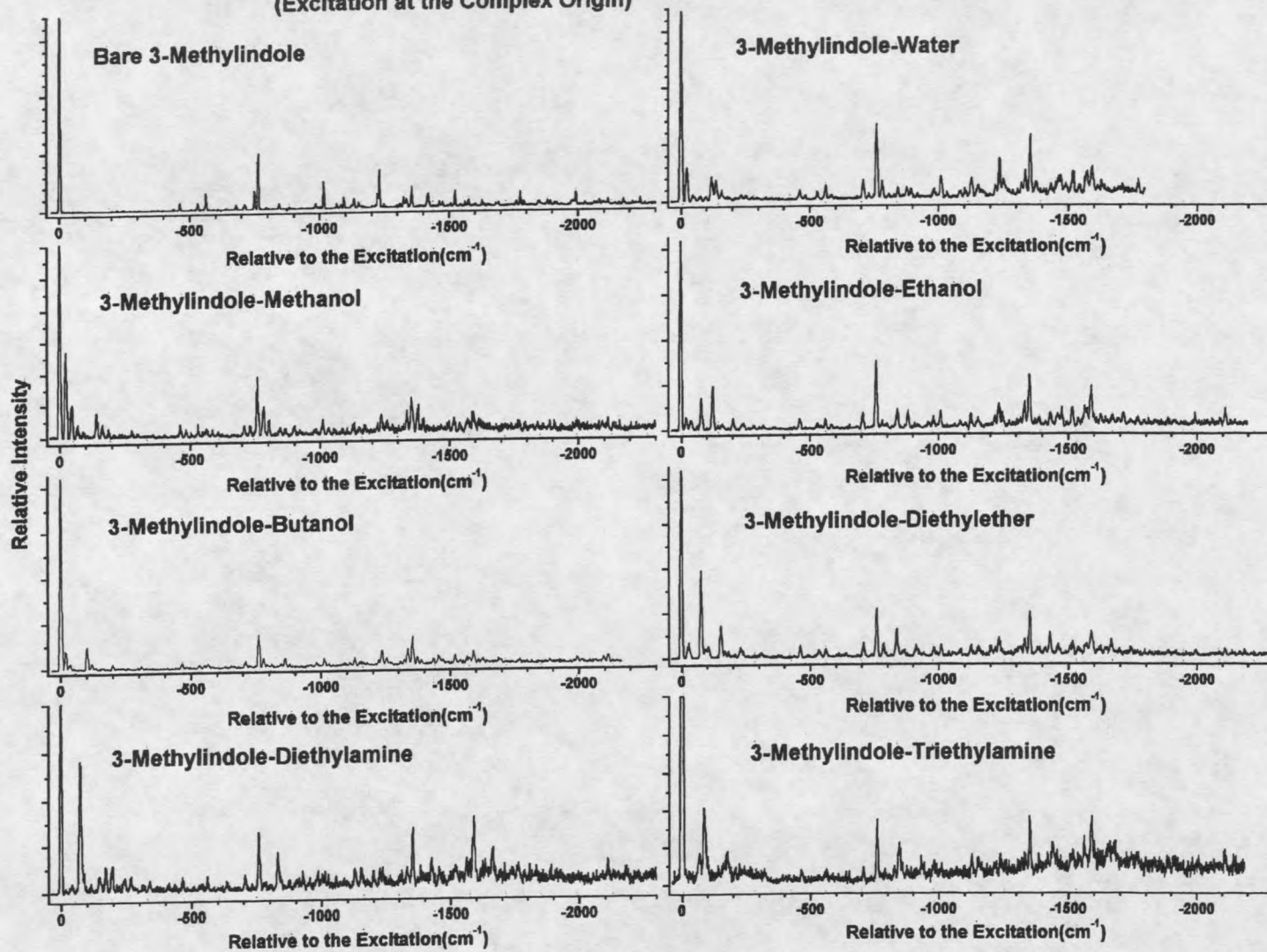


Figure 21. Dispersed fluorescence spectra are shown for bare 3-methylindole and for its complexes with various polar solvents. The monochromator resolution is about 8 cm^{-1} for bare 3-methylindole and about 14 cm^{-1} for the complexes.

Dispersed Fluorescence

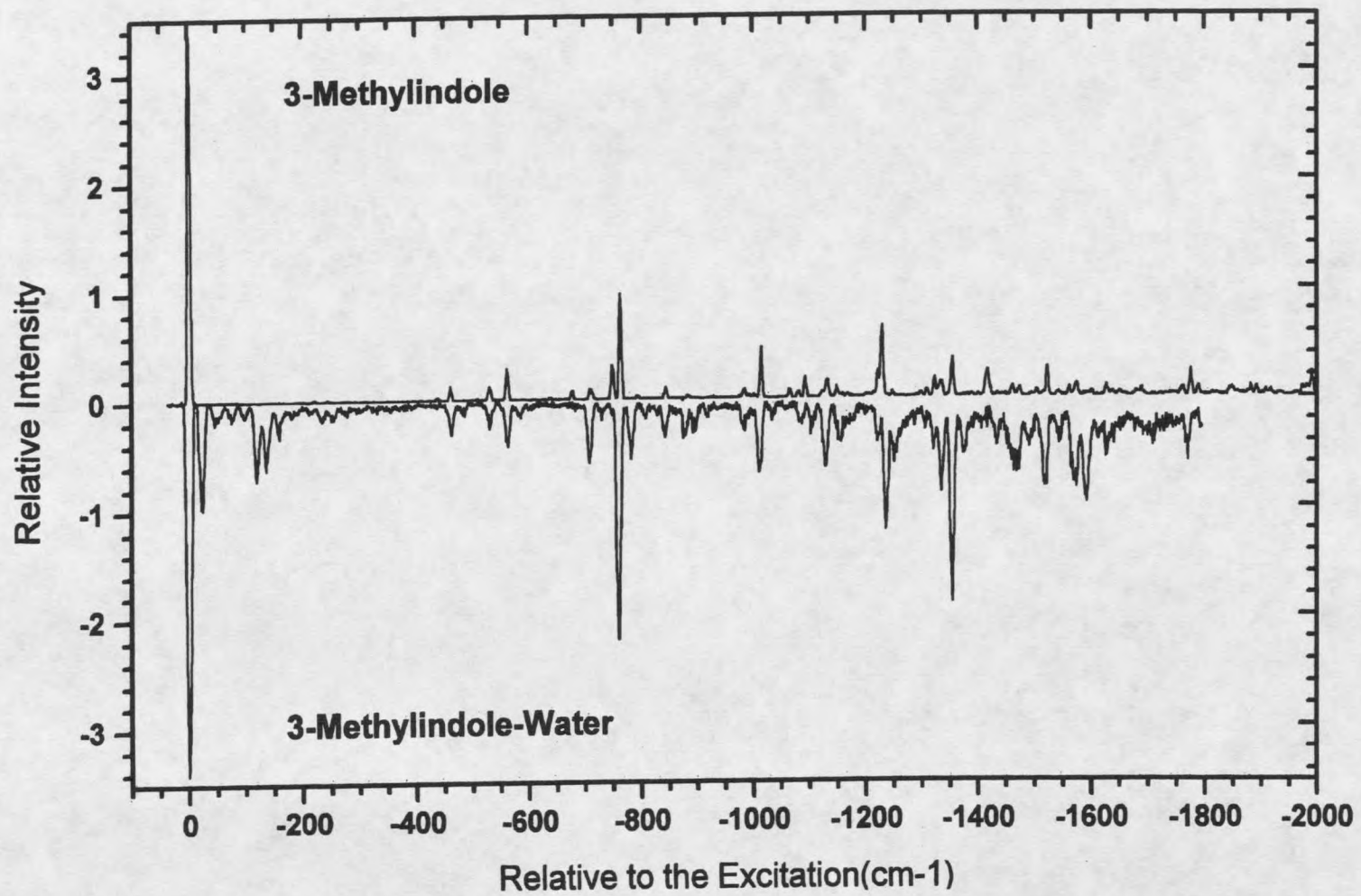


Figure 22. Dispersed fluorescence is shown for 3-methylindole and 3-methylindole-water. The monochromator resolution is about 8 cm⁻¹ for 3-methylindole and about 14 cm⁻¹ for 3-methylindole-water.

When 3-methylindole forms a complex with a polar solvent, the 1L_a state will be red-shifted relative to the 1L_b state(9). It is likely then that some understanding of this shift will be gained by considering the Ω -values of similar vibronic transitions in the different complexes. Consider first the peak at 117 cm^{-1} in the water complex (Figure 23), 136 cm^{-1} in the methanol complex (Figure 24), and 129 cm^{-1} in the ethanol complex (Figures 19 and 25). For all three complexes the Ω -value suggests 1L_b character and is similar to the value observed for the bare 3-methylindole origin. It is possible that these peaks represent the position of the 1L_b origin for these three complexes. The triethylamine complex has no similarly located peak with a large Ω -value. This suggests that the 1L_a state is more red-shifted, relative to the 1L_b state, in the triethylamine complex than in the other three.

Moving from the origin to higher energy in the water, methanol, and ethanol complexes the Ω -value goes up and then starts to go down again. The Ω -value for the 223 cm^{-1} peak in the water complex(1.13) is much higher than those for the 230 cm^{-1} methanol peak(0.60) and 224 cm^{-1} ethanol peak(0.67). This suggests that the 1L_a origin in the methanol and ethanol complexes may be at an energy lower than the 1L_a origin in the water complex. For the triethylamine complex the Ω -value starts low and only starts to rise slightly starting with the 260 cm^{-1} peak. This would imply that the 1L_a and 1L_b states probably do not overlap very much in this complex. Finally, the presence of peaks with low Ω -values both above and below a peak with a higher Ω -value in the methanol and ethanol complexes, suggests a splitting of the 1L_a origin by the nearby 1L_b state. This is comparable to the situation in the bare 3-methylindole(51) where the 1L_a origin appears to be spread over a region of at least 140 cm^{-1} , starting near 334 cm^{-1} .

Two-Photon Excitation 3-Methylindole-Water

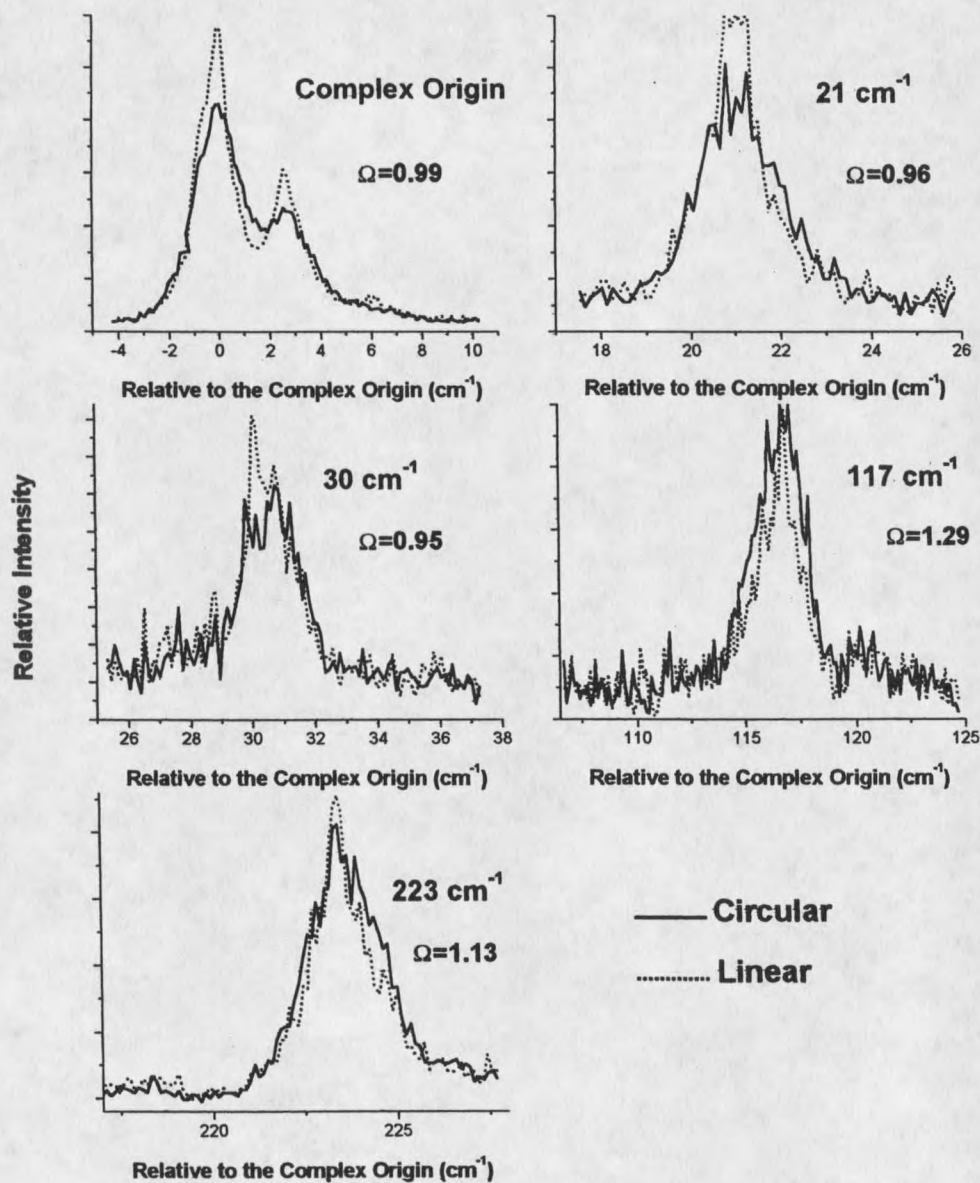


Figure 23. Polarized two-photon excitation spectra for different vibronic levels of the 3-methylindole-water complex are shown. The Ω -values are given in each spectrum.

Two-Photon Excitation 3-Methylindole-Methanol

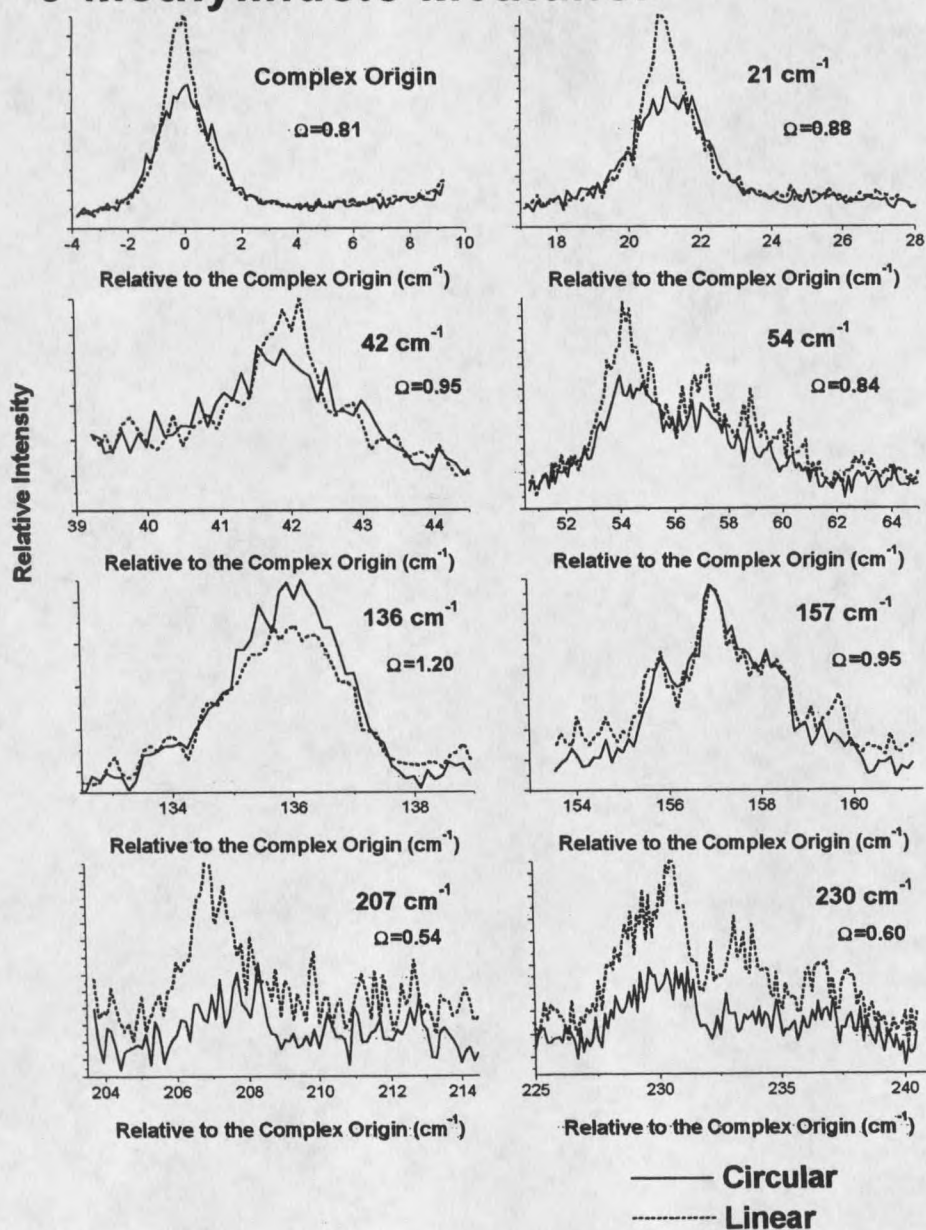


Figure 24. Polarized two-photon excitation spectra for different vibronic levels of the 3-methylindole-methanol complex are shown. The Ω -values are given in each spectrum.

Two-Photon Excitation 3-Methylindole-Ethanol

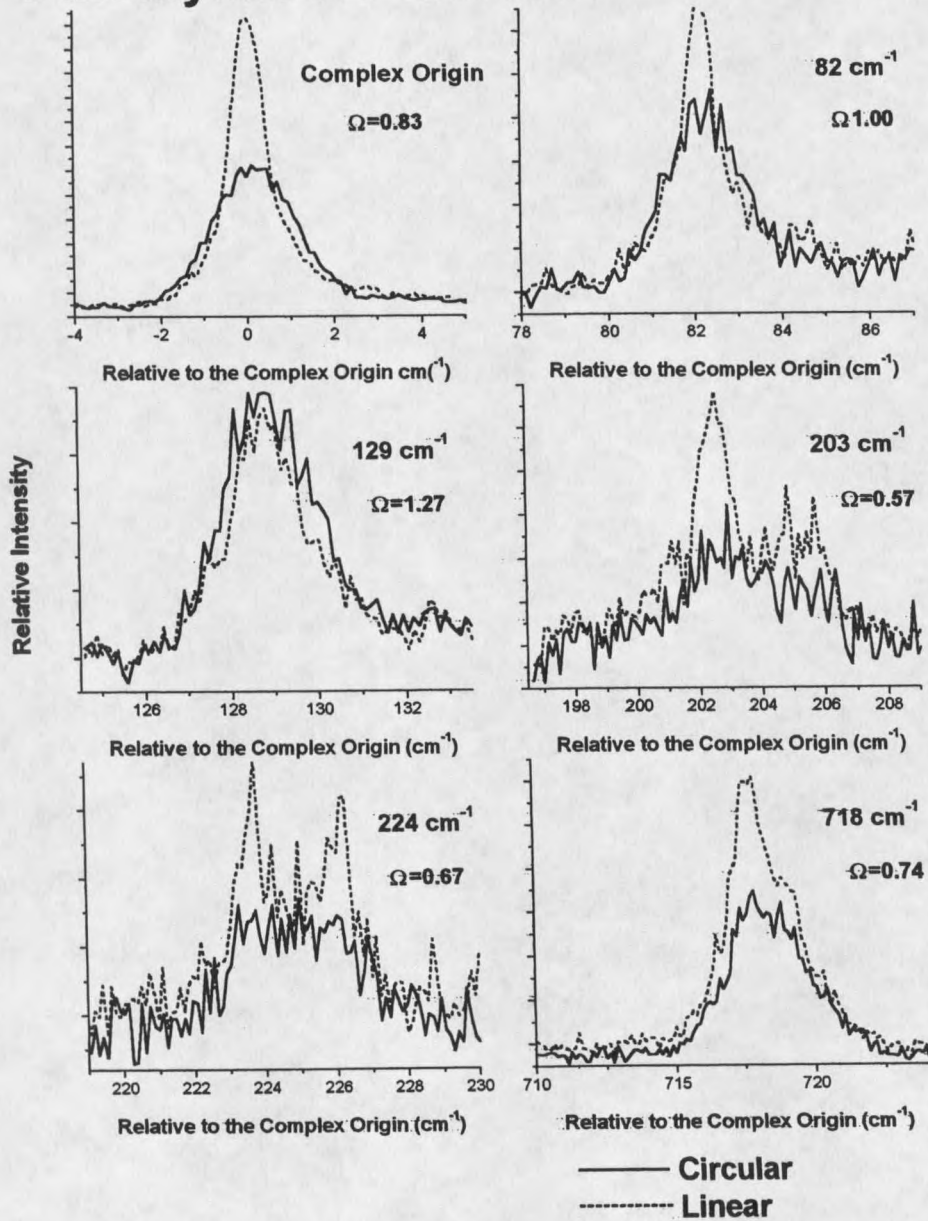


Figure 25. Polarized two-photon excitation spectra for different vibronic levels of the 3-methylindole-ethanol complex are shown. The Ω -values are given in each spectrum.

